JOURNAL OF GEOPHYSICAL RESEARCH, VOL. 99, NO. B8, PAGES 15,399–15,421, AUGUST 10, 1994

# Hunting for azimuthal anisotropy beneath the Pacific Ocean region

Yang Yu and Jeffrey Park

Department of Geology and Geophysics, Yale University, New Haven, Connecticut

**Abstract.** Lateral variations in azimuthal anisotropy cause significant waveform anomalies in long-period surface waves ($f < 15$ mHz, $T \gtrsim 70$ s), as a result of coupling between fundamental branch Rayleigh and Love waves. These anomalies, termed "quasi-Love" ($QL$) waves, have elliptical polarization, arrive slightly behind the Love wave but prior to the Rayleigh wave, and are observed on many propagation paths in the Pacific Ocean region. Our observations of quasi-Love waves indicate the existence of strong lateral anisotropic gradients in the western Pacific Ocean, in particular, near Hawaii and seaward of the Tonga-Kermadec, Kurile and Marianas-Izu-Bonin subduction zones. A lack of quasi-Love generation beneath the Phillipine Sea suggests weak azimuthal anisotropy in the region. In the southwest Pacific Ocean, the long-period quasi-Love waveforms recorded at station SNZO (South Karori, New Zealand) can be fit well with a simple anisotropic Earth model with a 90° rotation in the orientation of the fast $P$ velocity axis near the boundary between the Indo-Australian and the Pacific plates. In this model, 6% $P$ wave velocity anisotropy from the Moho to 210 km depth, with a NNE-SSW fast direction (roughly parallel to the plate boundary), extends 500-1000 km east of the Tonga-Kermadec trench, where it shifts to a WNW-ESE orientation (parallel to fracture zones in the southernmost Pacific plate). This solution is nonunique, however, as a similar lateral variation of 2% $S$ wave anisotropy at asthenospheric depths (100–300 km) generates similar waveform anomalies. We attribute the laterally varying anisotropy to either (1) flow variations in the asthenosphere, consistent with lateral shear detected in deep Tonga-Kermadec seismicity, (2) variations in fossil spreading direction in the Cretaceous long normal polarity interval, (3) the disturbance of fossil anisotropy caused by the passage of the Louisville Ridge hotspot, and (4) lithospheric compression associated with continental collision along the Alpine Fault. The apparent location of the Love-to-Rayleigh "scatterer" favors options 1 and 3. Gradients in azimuthal anisotropy are inferred in the northwestern Pacific, associated with one or more of these mechanisms. A quasi-Love wave observed on a path from Alaska to PPT (Papeete, Tahiti) is bandlimited to $f > 8$ mHz, suggesting lateral variations with wavelength twice the spacing of fracture zones in the north central Pacific.

## Introduction

Global tomographic models of isotropic seismic velocity variations have significantly improved our knowledge of the Earth's upper mantle structure [*Woodhouse and Dziewonski,* 1984; *Masters,* 1989; *Tanimoto,* 1990; 1991; *Su and Dziewonski,* 1991; *Woodward and Masters,* 1991; *Zhang and Tanimoto,* 1993]. Several more recent tomographic studies have included azimuthal variations in Rayleigh and Love phase velocities [e.g., *Nishimura and Forsyth,* 1989; *Montagner and Tanimoto,* 1990; 1991]. There are, however, many anomalies in seismic records that are not satisfactorily explained by these models.



Paper number 94JB00936.
0148-0227/94/94JB-00936$05.00

In a spherical Earth, seismic motion can be separated into spheroidal and toroidal motions. Toroidal modes ${}_nT_l$ sum to form Love waves, which appear primarily on the transverse component of seismic records. Spheroidal modes ${}_nS_l$ sum to form Rayleigh waves, which appear primarily on the vertical and radial components. The Earth's asphericity, however, can couple the two types of free oscillation into hybrid motion. As a result, "quasi-Love" waves may appear on the vertical and radial components and "quasi-Rayleigh" waves on the transverse component. Spheroidal-toroidal coupling due to rotational Coriolis force is responsible for very-long-period quasi-Love waves with $f \lesssim 4$ mHz [*Park and Gilbert,* 1986; *Park,* 1986; *Masters et al.,* 1983]. At much shorter periods, the strong coupling of higher-mode Rayleigh and Love waves can be caused by azimuthal anisotropic structure, resulting in significant particle motion polarization anomalies [*Kirkwood and Crampin,* 1981a, b; *Kawasaki and Koketsu,* 1990]. These

latter studies, however, are based on the modeling of wave motion in an anisotropic plane-stratified medium and are restricted to $f \gtrsim 30$ mHz ($T < 35$ s). *Park and Yu* [1992; 1993] and *Yu and Park* [1993] predicted that strong waveform anomalies associated with fundamental Rayleigh-Love coupling can be generated by anisotropic upper mantle structure. We identified 4–20 mHz waveform anomalies (periods 50–250 s) of this type in several data examples for both oceanic and continental propagation paths. These modeling studies suggest the feasibility of using long-period waveform anomalies to study regional tectonic processes.

In this study we investigate long-period ($f \lesssim 15$ mHz, $T \gtrsim 70$ s) surface waves that propagate in the Pacific Ocean region in order to determine the anisotropic properties of the underlying upper mantle and to understand how the anisotropic structure might be caused by tectonic processes. We first present examples of quasi-Love waves observed in the Pacific Ocean region to illustrate their distinguishing properties. Based on the theoretical modeling of surface wave propagation in simple Earth models, we show in detail how waveform anomalies might be related to anisotropic structure of the upper mantle. We then interpret our quasi-Love wave observations in terms of simple anisotropic models and discuss what seismological and tectonic inferences can be made from the data.

## Quasi-Love Waves and Anisotropy

### Quasi-Love Waves in the Data

Love-to-Rayleigh or Rayleigh-to-Love conversion is a common behavior of surface wave propagation in the real Earth. Figure 1a shows long-period seismic data recorded at station SNZO (South Karori, New Zealand) after the November 8, 1980, strike-slip $M_S = 7.2$ earthquake near Eureka, California (epicenter 41.12°N, 124.25°W, $d = 19$ km, according to the National Earthquake Information Center (NEIC)). Love/toroidal motion dominates the records because station SNZO is near the Rayleigh wave radiation node of the strike-slip source. The synthetic seismogram calculated from a spherical reference Earth model is shown for comparison (Figure 1b). Although real data are more complicated, the fundamental Love wave packet ($G_1$) and Rayleigh wave packet ($R_1$) are readily identified in the low-passed record. Note the wave packet on the vertical and radial components that lags slightly the arrival of $G_1$ and leads the arrival of $R_1$ (Figure 1a). Comparison with spherical Earth synthetics indicates that, at $f < 15$ mHz, no overtone energy arrives in the time window where the waveform anomaly arrives. Studies of long-period surface wave and body wave data [e.g., *Lay et al.*, 1982] do not show source complexity that could be used to explain this waveform anomaly. The fact that waveform anomalies appear on both radial and vertical components and are poorly coherent with the Love wave suggest that the anomalies are not simply caused by Love wave refraction away from the source-receiver great circle, which could be generated by the coupling between toroidal modes [*Woodhouse and Wong*, 1986; *Park*, 1986]. We identify the anomalous waveform as a quasi-Love ($QL$) wave, generated by Rayleigh-Love coupling that transfers energy from transverse (Love) motion into radial-vertical (Rayleigh) motion. Quasi-Love waves with $f \lesssim 4$ mHz can be generated by rotational Coriolis force [*Park and Gilbert*, 1986; *Park*, 1986]. Typical $QL$ waves in real data (Figure 1a) have spectral content that cannot be explained by Earth rotation, so that other aspherical Earth structure must be responsible. We show below that azimuthal anisotropy in the Earth's upper mantle is a most likely explanation.

The quasi-Love wave shown in Figure 1 is not unique. Similar $QL$ wave packets are consistently observed at station SNZO for events along the west coast of North America (Figure 2). Propagation paths in the southwest Pacific Ocean for these records are similar, though the magnitudes and source locations differ. Note that the anomalous $QL$ waveforms, unlike the Rayleigh wave packet $R_1$, are quite similar in all the records. Quasi-Rayleigh ($QR$) waveforms, due to Rayleigh-to-Love conversion, are also observed at SNZO for similar propagation paths, but different source mechanisms. Figure 3a shows seismic motion recorded at station SNZO for the August 4, 1985, central California earthquake. Rayleigh/spheroidal motion dominates the record because station SNZO is near the Love wave radiation node of the event. The $QR$ waveform anomaly arrives after $G_1$ on the transverse component record. The $QR$ anomaly arrives prior to $R_1$, and we confirmed that its polarization is incoherent with $R_1$ by using frequency-dependent polarization analysis [*Park et al.*, 1987; *Park and Yu*, 1992].

Quasi-Love waves in the data are strongly dependent on the source-receiver path. Figure 3b shows the long-period seismic record at station SNZO for a strike-slip event on the Mid-Indian Ridge (NEIC epicenter 36.82°S, 78.49°E, $d = 10$ km). The receiver is close to the Rayleigh wave radiation node, so that Love/toroidal motion dominates the record. In contrast to Figure 1, the vertical component record shows no waveform anomalies before $R_1$. Note that some energy appears on the radial component coeval with the Love wave packet $G_1$. The timing and polarization of this waveform is consistent with Love refraction in the horizontal plane. We observed little evidence for $QL$ waves at SNZO for several similar events on the Mid-Indian Ridge. The fact that both strong and weak waveform anomalies are observed at this single station argues against the possibility of bad instrument recording conditions, such as a tilted seismic sensor or site effects.

Quasi-Love waves are composed of Love-to-Rayleigh scattered energy, and so have elliptical polarization in the vertical-radial plane. Figure 4a shows the phase relationship between vertical and radial components at SNZO. The anomalous waveform shows elliptical

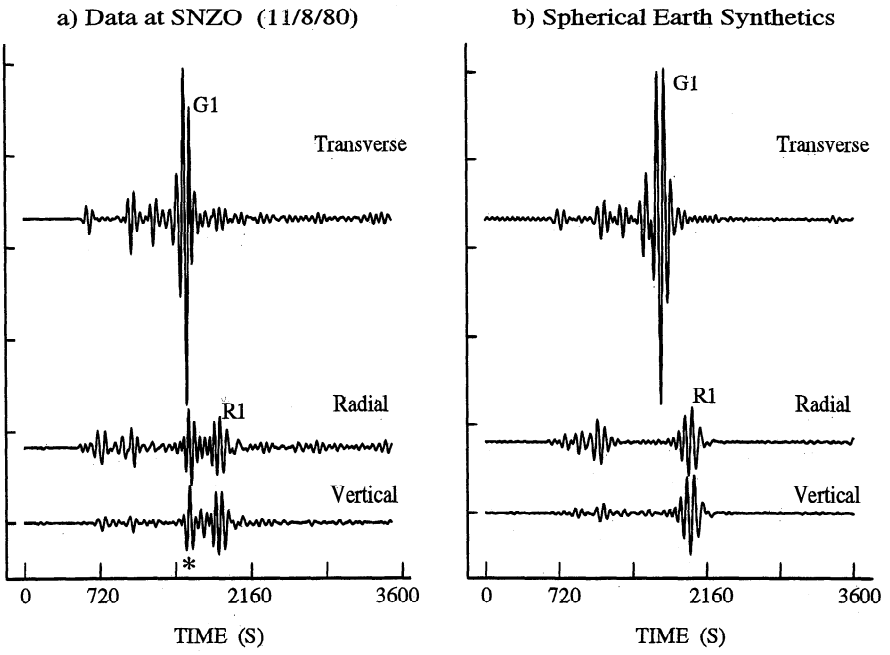


**Figure 1.** (a) LP-channel motion recorded at station SNZO (South Karori, New Zealand) for the November 8, 1980, earthquake near Eureka, California ($M_S = 7.2$). Horizontal data are rotated to the radial and transverse directions. The data are low-passed at 15 mHz. G1, the first wave packet of fundamental Love waves; R1, the first wave packet of fundamental Rayleigh waves. The asterisk marks the quasi-Love ($QL$) waveform anomaly. (b) Synthetic seismograms calculated from a spherical Earth model (oceanic PEM) for the Eureka-SNZO path. The synthetics include all fundamental and overtone free oscillations below the frequency cutoff $f_c = 15$ mHz.

(Rayleigh) particle motion, except at the beginning, where the radial component may have experienced some refracted Love motion. The $QL$ wave in the VH-channel record from KIP (Kipapa, Hawaii) for the July 16, 1990, Philippine event exhibits purely elliptical polarizations, apparently without Love refraction effects (Figure 4b).

Quasi-Love waves may arrive anytime between the main Love wave packet $G_1$ and the Rayleigh wave packet $R_1$. As examples, we show the long-period seismic data from the central Pacific station KIP for the April 23, 1992, Burma-China border event (Figure 5a) and the VH-channel seismic record at Geoscope station INU (Japan) for the June 18, 1988, strike-slip event in the Gulf of California (Figure 5b). Both records show strong waveform anomalies. However, the waveform that we identify as a quasi-Love wave (Figure 5a) arrives in a relatively wide time window and is not, like $QL$ at INU (Figure 5b), separated from the Rayleigh wave packet $R_1$. In addition, many examples suggest that quasi-Love wave anomalies are strongly frequency-dependent. The variety of examples demonstrates that the details of $QL$ waveforms differ for different source-receiver paths and suggests that careful modeling is necessary to relate the data to plausible aspherical structure in the Earth.

## Theoretical Modeling of Quasi-Love Waves

The data presented above illustrate the presence of quasi-Love anomalies in many long-period seismic records for surface waves propagating in the Pacific Ocean region. What is responsible for such waveform anomalies and what do quasi-Love waves tell us about the Earth's structure?

**Isotropic and anisotropic models.** The coupling of spheroidal and toroidal free oscillations due to the Earth's asphericity should be responsible for the observed Rayleigh-Love scattering effects. In order to understand better the upper mantle structure responsible for the quasi-Love waveforms described above, we model long-period surface wave propagation using simple anisotropic models. We also compare these with laterally varying isotropic models to demonstrate how difficult it is to generate quasi-Love waves without anisotropy. *Park and Yu* [1992] and *Yu and Park* [1993] have modeled smoothly varying anisotropic structure in the upper mantle to explain quasi-Love waves observed prior to the second Rayleigh wave packet $R_2$. An extension of the Born perturbation algorithm has also been developed by *Su et al.* [1993] to model more general structures and has been used successfully to retrieve simple anisotropic models in synthetic inversion experiments. The global data set, however, contains many impulsive $QL$ waveforms prior to $R_1$, suggesting sharper gradients in the Earth's structure. We choose oceanic PEM (Preliminary Earth Model) of *Dziewonski et al.* [1975] as the spherical Earth reference model, and limit the perturbation to spherical caps poleward of $\pm 45°$ latitude, indicated schematically by the dark

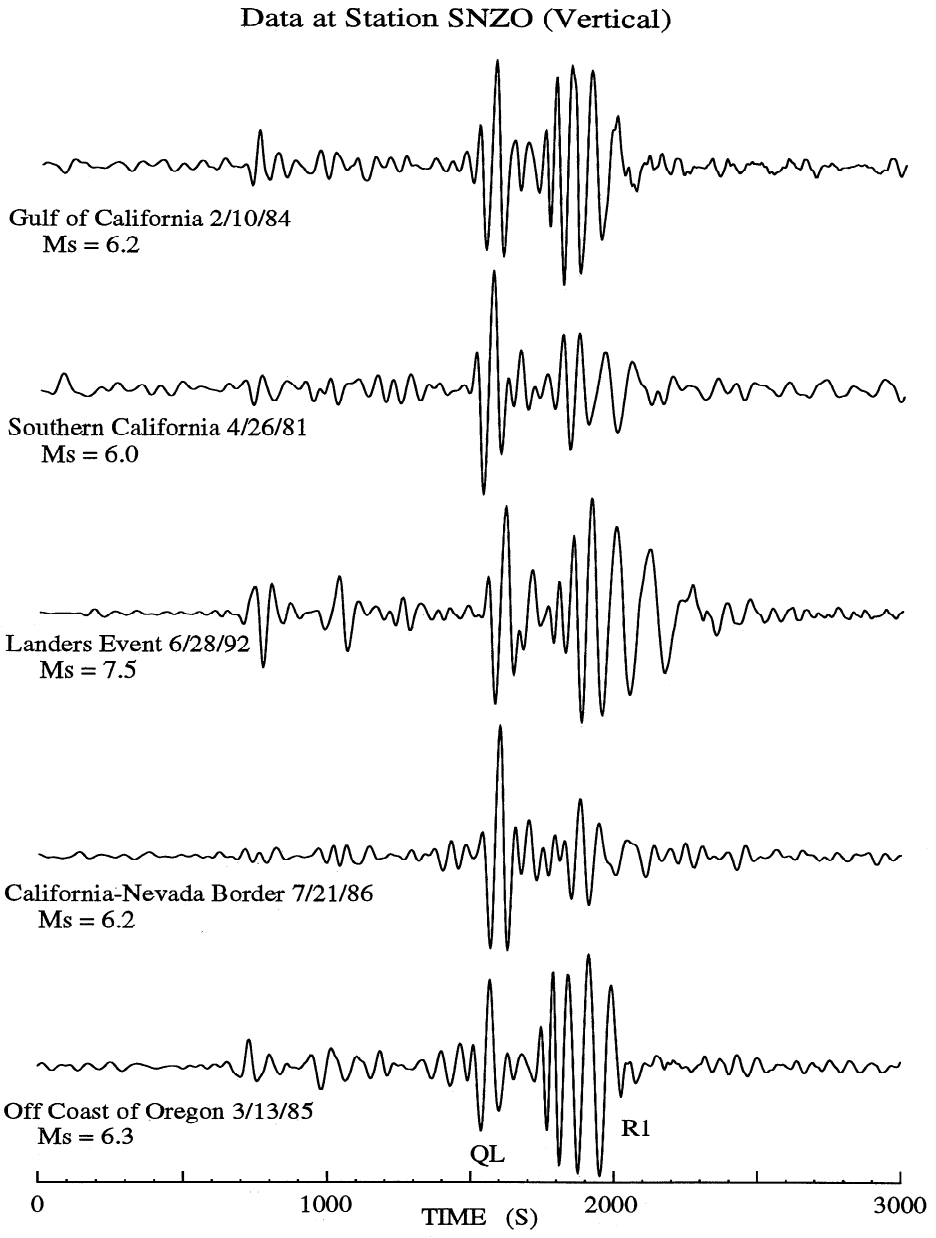


**Figure 2.** Vertical component seismic data recorded at station SNZO for five large earthquakes along the west coast of North America. The data are low-passed at 15 mHz. $QL$ marks the quasi-Love waves.

color (Figure 6). For simplicity, let us assume that the fractional velocity perturbation in the block is constant in a layer from the Moho (11 km) to 210 km depth in the upper mantle. We assume that material in the perturbed region has a horizontal symmetry axis (azimuthal anisotropy). In the spherical polar basis of $\{\hat{\theta}, \hat{\phi}, \hat{\mathbf{r}}\}$, we use an angle $\xi$ to specify the orientation of the symmetry axis in the $\theta\phi$ tangent plane. The angle $\xi$ is measured counterclockwise from $\hat{\theta}$ to the symmetry (fast $P$ wave) axis, that is, counterclockwise from south. Seismic velocity perturbations for plane $P$ and $SV$ waves that propagate at an angle $\eta$ from the symmetry axis depend on the formulas [*Backus*, 1965; *Crampin*, 1977; *Shearer and Orcutt*, 1986; *Park and Yu*, 1992]

$$\begin{aligned} \delta(\alpha^2)/\alpha_0^2 &= A + B\cos 2\eta + C\cos 4\eta \\ \delta(\beta^2)/\beta_0^2 &= D + E\cos 2\eta. \end{aligned} \tag{1}$$

where $\alpha$ and $\beta$ are the $P$ and $S$ wave velocities. For the isotropic model ($B = C = E = 0$), we prescribe peak-to-peak variations of 4% in $\alpha$ ($A = 0.04$) and 6% in $\beta$ ($D = 0.06$). In the anisotropic model, we choose the symmetry axis shown by the black arrow ($\xi = 90°$) in Figure 6. We choose perturbation parameters $B = 0.06$, $A = C = D = E = 0.00$, corresponding to 6% peak-to-peak azimuthal variation in $P$ velocity ($2\eta$ term) and no perturbation to $S$ wave velocity. The long-period seismic responses for these models are calculated with the modal summation technique [*Park and Yu*, 1992; *Yu and Park*, 1993]. We include the effects of

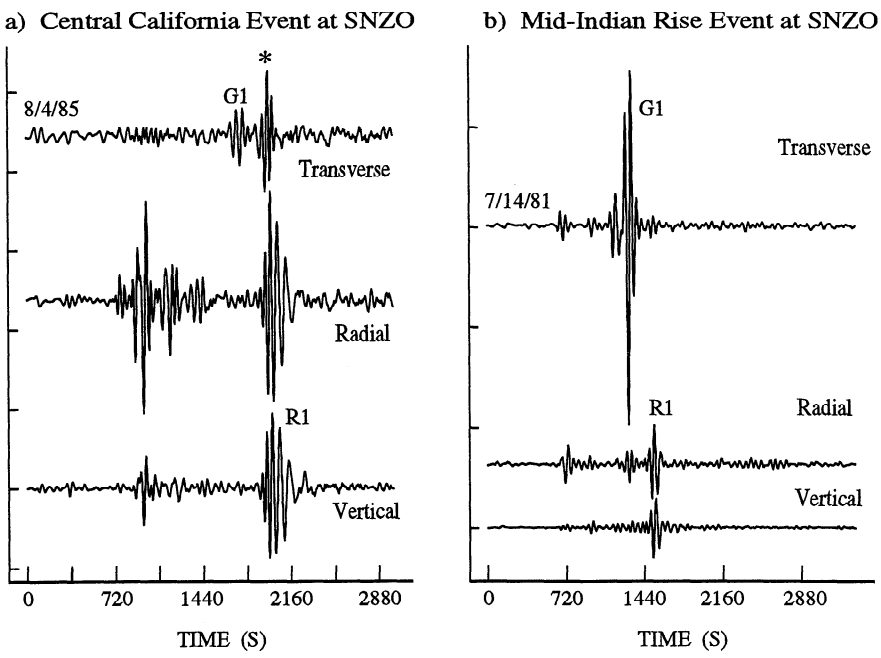


**Figure 3.** (a) LP-channel motion recorded at station SNZO for the August 4, 1985, central California earthquake ($M_S = 5.9$). The asterisk marks the quasi-Rayleigh ($QR$) waveform anomaly. (b) LP-channel motion recorded at station SNZO for the July 14, 1981, Mid-Indian Rise event ($M_S = 6.0$). Both records are low-passed at 15 mHz.

Earth rotation and hydrostatic ellipticity in our modeling. The real Earth is, naturally, more complicated than these models. However, our calculations demonstrate important propagation behaviors of long-period surface waves, which can be used to interpret the observed $QL$ waveform anomalies.

Figure 7 shows synthetic seismograms summed from the fundamental spheroidal and toroidal free oscillations with frequencies $f \leq 15$ mHz. A source is located at site 1 and a station at site 2 in the perturbed region shown in Figure 6. The surface waves travel first in the laterally homogeneous isotropic medium, then cross the sharp boundary near the station, which could be isotropic-to-isotropic or isotropic-to-anisotropic. Figure 7a shows long-period seismic waveforms for an isotropic perturbation in the shaded region. There is no significant waveform anomaly on the vertical component prior to $R_1$. However, the radial component shows energy coherent with the Love wave, due to the refraction of the Love wave off the source-receiver great circle. The sharp jump in $S$ wave velocity induces substantial coupling between toroidal free oscillations, which contributes to the refraction. Similar surface wave refractions are often observed in the data (e.g., Figure 3b). In contrast, long-period seismic waveforms for an anisotropic perturbation exhibit a quasi-Love anomaly, on both vertical and radial components, that lags the arrival of the Love wave (Figure 7b). Spheroidal-toroidal (Rayleigh-Love) coupling is responsible for the anomalous waveform. Our other experiments [*Yu and Park*, 1993] have suggested that significant quasi-Love waves are very difficult to generate with the level of isotropic velocity perturbation consistent with global tomographic mantle models, such as M84A [*Woodhouse and Dziewonski*, 1984]. The experiment with spherical cap models suggests that simple sharp gradients in isotropic structure, as might occur at continent-ocean boundaries, are also weak contributors to $QL$ observations.

Figure 8a shows radial motion in detail for the anisotropic model. The waveform anomalies are similar to anomalies in the data at KIP (Figure 4b). Note the 90° phase delay between vertical and radial components of the waveform anomalies, indicating that the quasi-Love wave, like the Rayleigh wave, has purely elliptical polarization. There is no Love wave refraction on the radial component in Figure 8a, because the $P$ wave velocity perturbation in $B$ ($2\eta$ term) does not induce coupling between toroidal modes [*Park*, 1993]. However, $S$ wave velocity anisotropy (scaled by $E$) can generate both a quasi-Love wave and Love wave refraction. As an example, Figure 8b shows seismic motion for a model with 2% azimuthal variation in $S$ wave velocity ($A = B = C = D = 0$, $E = 0.02$). The late part of the $QL$ wave shows elliptical polarization as expected. However, the polarization of its initial part is not elliptical because the radial component is a combination of quasi-Love and refracted-Love waves. Similar behaviors are observed in the data, such as in Figure 4a.

**Effects of the location of anisotropic structure.** The effects due to near-receiver and near-source structure can be investigated in our simple models by comparing the synthetics calculated for different source-receiver pairs. The quasi-Love wave arrives closely behind the Love wave and is separated from the Rayleigh

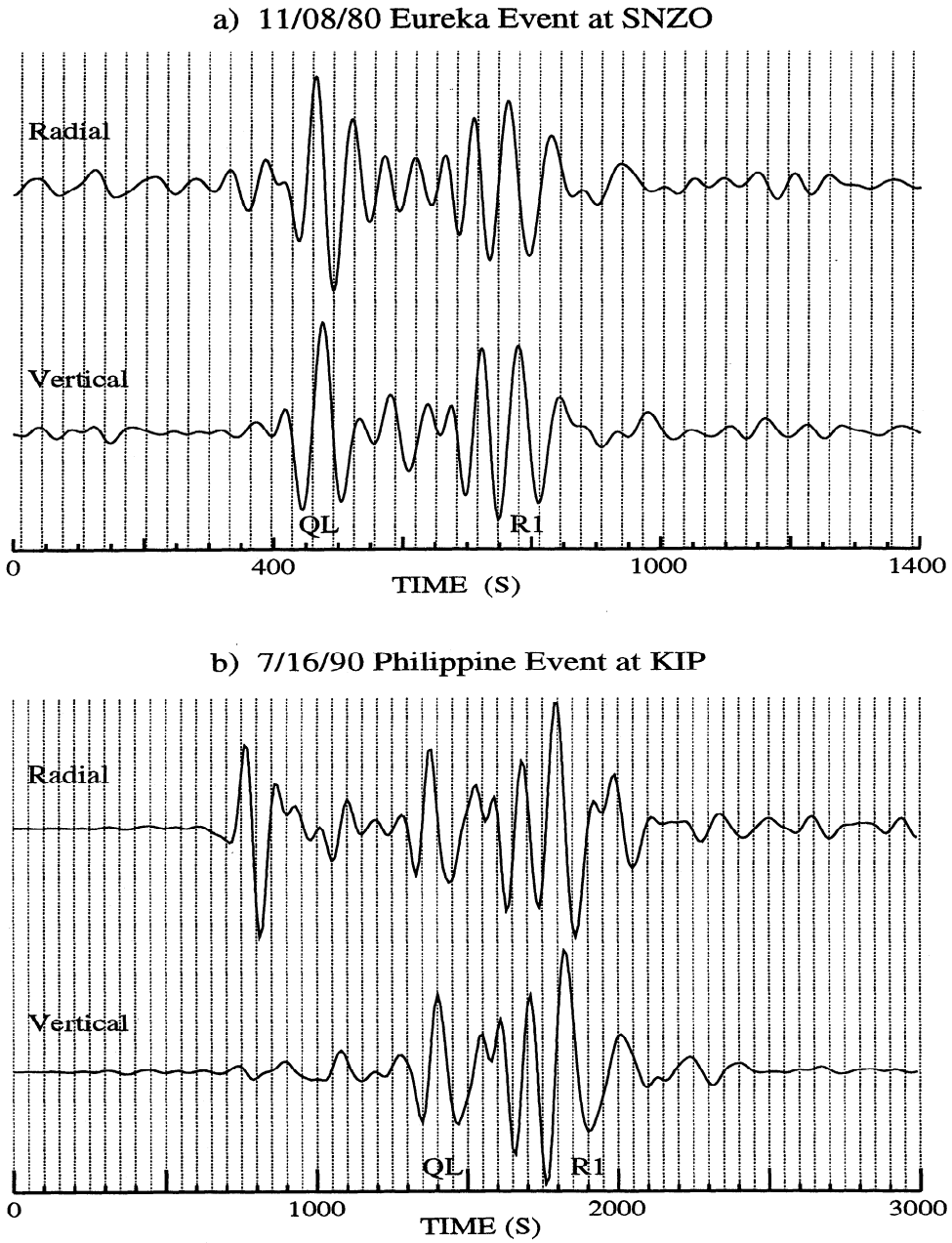


**Figure 4.** (a) Vertical and radial component seismic data recorded at station SNZO for the November 8, 1980, Eureka event. (b) Vertical and radial component seismic data recorded at station KIP (Kipapa, Hawaii) for the July 16, 1990, Philippine event ($M_S = 7.8$, NEIC epicenter 15.66°N, 121.23°E, $d = 25$ km). The data are low-passed at 12 mHz. Vertical dashed lines are plotted for comparing the phase delay between components.

wave packet in Figure 7b. For that source-receiver pair (source at site 1, receiver at site 2), the station is close to the anisotropic gradient and the quasi-Love wave is generated near the receiver. Figure 9 shows synthetics for a source at site 1 and a receiver at site 3. The perturbation is near the midpoint of the propagation path (see Figure 6). The isotropic model (Figure 9a) shows weak very-long-period energy before Rayleigh wave packet, due to mixed-type coupling caused by Earth rotation [*Park*, 1986]. On the radial component, there is energy coherent with the Love wave, due to Love wave refraction. For the anisotropic model (Figure 9b), on the other hand, only weak very-long-period energy, caused by Earth rotation, arrives closely with the Love wave packet. However, a well-dispersed $QL$ wave on the vertical and radial components arrives far behind the Love wave because the anisotropic gradient is located at the midpoint of the path. Figure 10 shows the synthetic waveform for an event at site 2 just beyond the lateral interface, with the receiver at site 3. Again, there is no significant quasi-Love wave for the isotropic model (Figure 10a), though the effect of slight Love wave refraction can be found on the radial component. For the anisotropic model (Figure 10b), a quasi-Love wave

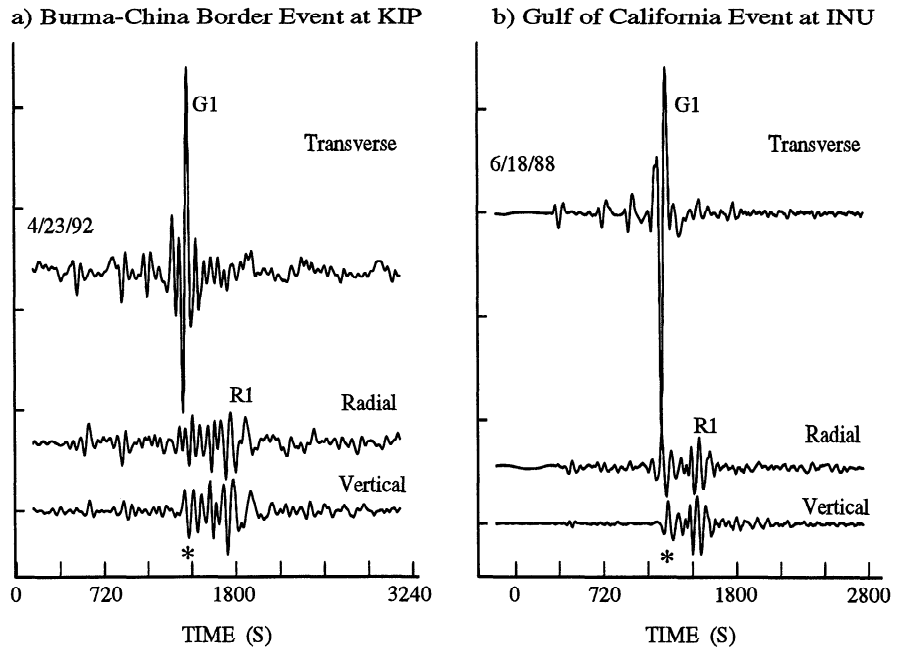


**Figure 5.** (a) LH-channel motion recorded at station KIP for the April 23, 1992, Burma-China border event ($M_S = 6.3$, NEIC epicenter 22.36°N, 98.86°E, $d = 33$ km). The data are low-passed at 18 mHz. (b) VH-channel motion recorded at Geoscope station INU (Japan) for the June 18, 1988, Gulf of California event ($M_S = 6.9$). The data are low-passed at 15 mHz. Asterisks mark the waveform anomalies.

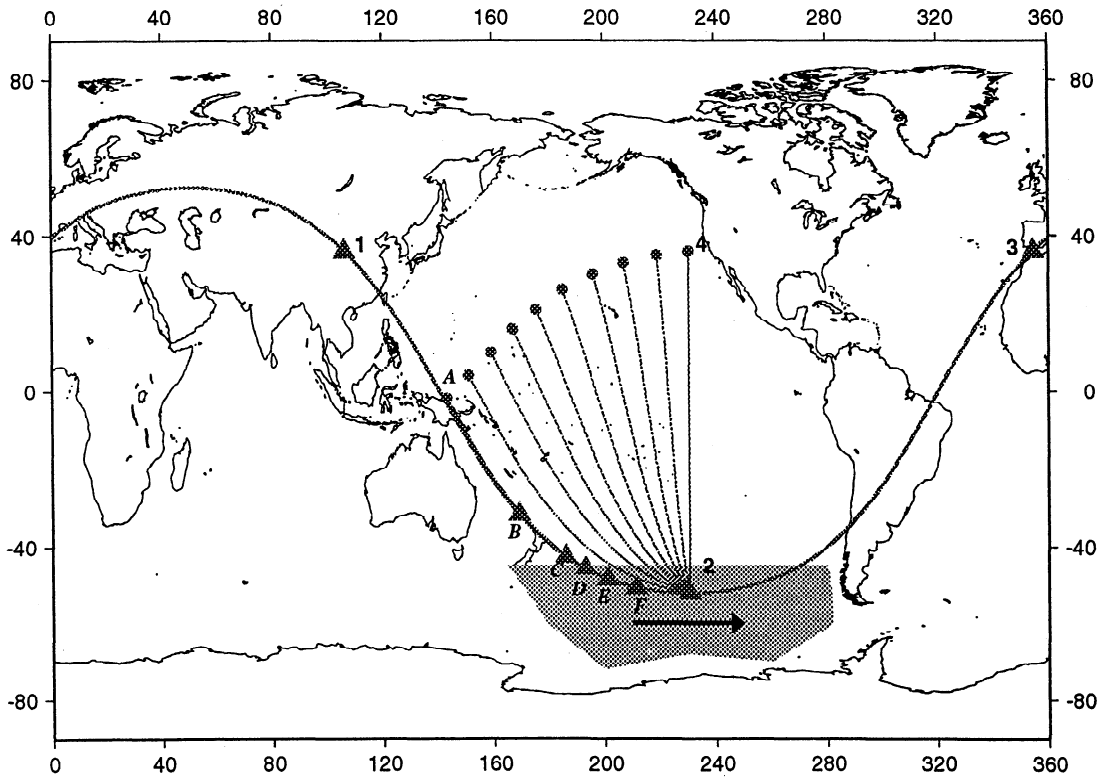


**Figure 6.** Simple Earth models used in modeling the propagation of long-period surface waves in an aspherical Earth. Seismic velocities are perturbed in a spherical cap indicated schematically by the shaded area, in a layer from 11 to 210 km depth in the upper mantle. The solid arrow shows the fast $P$ wave velocity direction when the perturbation structure is anisotropic. Circles and triangles mark source and/or receiver locations. Letters and numbers indicate the source and receiver locations referred to in the text. Also plotted are the great circle paths for which synthetic seismograms were constructed.

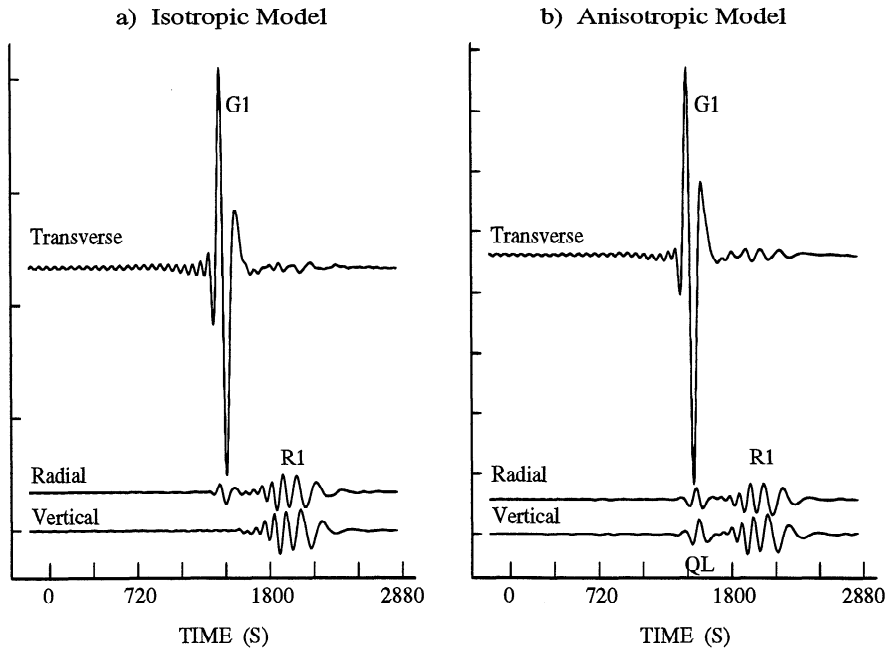


**Figure 7.** Coupled-mode synthetic seismograms for aspherical Earth models with sharp gradients close to the receiver. The source is located at Site 1 and receiver at Site 2 in the perturbed region (Figure 6). The synthetics include all fundamental spheroidal and toroidal modes to $f = 15$ mHz. (a) Synthetics for an isotropic Earth model. (b) Synthetics for an anisotropic Earth model.

is generated near the source and is difficult to observe since the waveform anomaly is hard to distinguish from $R_1$.

Can we infer, from relative arrival times, where the quasi-Love wave is generated? Figure 11 shows how the quasi-Love waveform is sensitive to the distance of the receiver from the anisotropic perturbation boundary. Synthetics are calculated with a fixed source (site 1, Figure 6) for several receivers (B, C, D, E, F and 2) along the same great circle path. There is no waveform anomaly at receiver B for surface waves propagating entirely within the isotropic structure. Weak energy arrival before $R_1$ at receiver C may be partially caused by off-path wave propagation near the sharp boundary. Practical limitations in our coupled-mode summation may also be partially responsible for the anomaly, as we only consider the interaction between free oscillations that are closely spaced in frequency. For a receiver within the anisotropic structure and very close to the perturbation boundary (receiver D and E), quasi-Love waves arrive closely behind the main Love wave. With increasing distance from the perturbation boundary, the quasi-Love wave arrives later, relative to the main Love wave. At receiver F (1600 km from the boundary), for example, quasi-Love wave is about 25 s behind the main Love wave. For a "sharp" lateral gradient fairly close to the receiver, the "arrival time" of a quasi-Love wave may help us infer where the Love-to-Rayleigh conversion takes place. For a model with smooth, widespread anisotropic structure, the quasi-Love wave is expected to show dispersed energy between the main Love and Rayleigh waves [*Park and Yu*, 1992; *Yu and Park*, 1993], and not a distinct wave packet.

**Effects of the orientation of anisotropic structure.** The details of quasi-Love waveforms can provide us information about the orientation of anisotropic structures in the mantle. We compare in Figure 12a the synthetics at a single station location (site 2 in Figure 6) for several events at back azimuths between 0° and −90°. The epicentral distance is same for all the paths. For a source at site 4 (back-azimuth 0°), surface waves cross the sharp boundary perpendicular to the fast axis of $P$ wave velocity, and the quasi-Love wave is visually absent. As the angle to the fast $P$ wave direction at the perturbation boundary decreases from 90° to ∼ 45°, the $QL$ wave grows and details of the waveform vary. Note that the relative arrival times between the $QL$ wave and $R_1$ varies in Figure 12a because of variations in the distance between the receiver and the anisotropic boundary.

Figure 12b shows how quasi-Love waves are sensitive to the orientation of the fast velocity axis. For a source at A and a receiver at 2 (Figure 6), the fast $P$ wave velocity direction in the perturbed block is rotated from south ($\xi = 0°$) to east ($\xi = 90°$). The orientation of the fast direction, relative to the propagation path, affects both the strength and detail of the quasi-Love waveform significantly. In general, weak waveform anomalies occur for surface waves propagating parallel to the symmetry axis. Similar conclusions were reached by *Kirkwood and Crampin* [1981a, b] in modeling short-period surface waves in an anisotropic plane-stratified medium.

**What can quasi-Love waves tell us about mantle anisotropy?** The results from theoretical modeling indicate that strong quasi-Love ($QL$) and quasi-

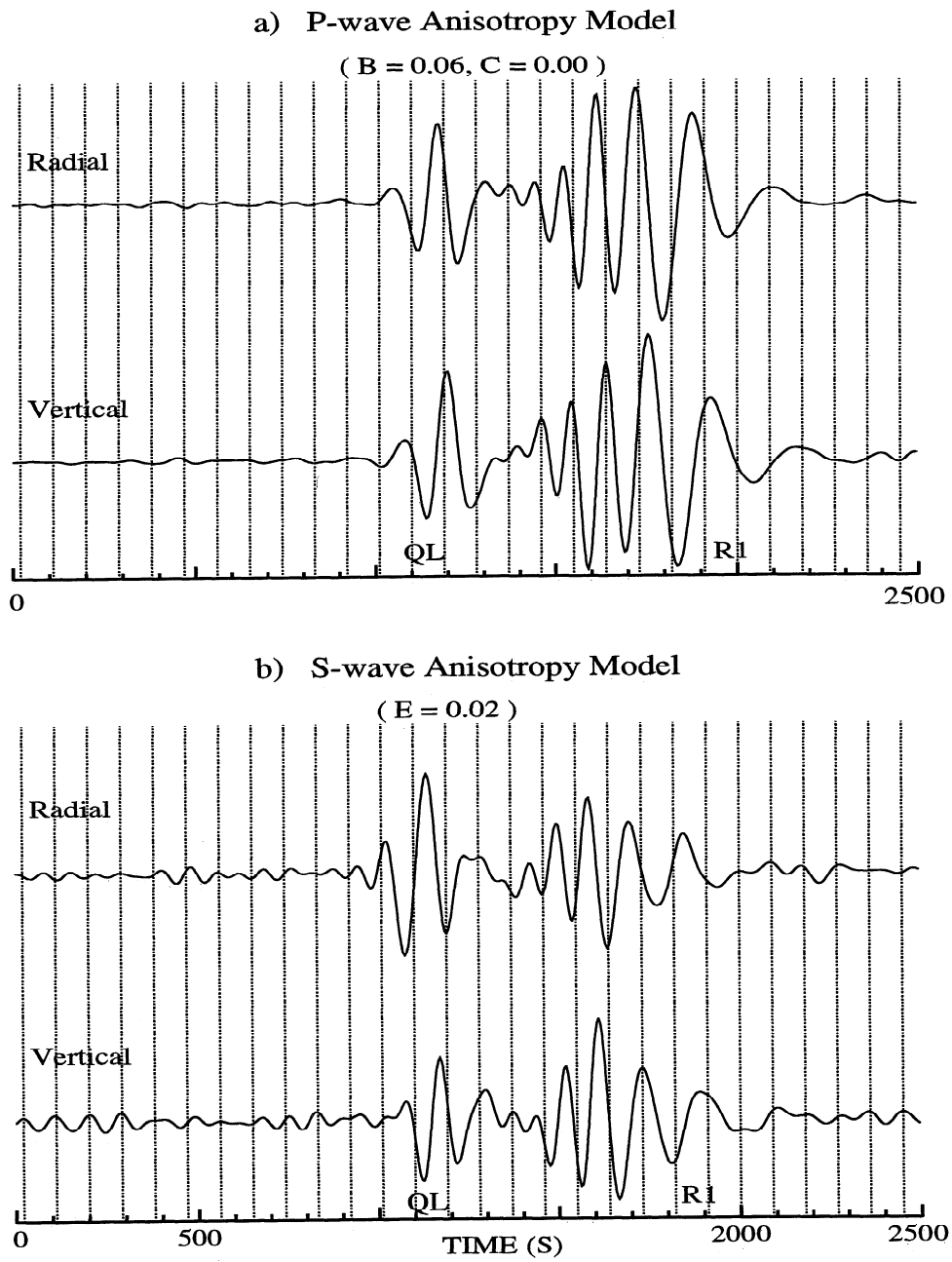


**Figure 8.** Vertical and radial component synthetic seismograms for two anisotropic Earth models. The source is located at Site 1 and receiver at Site 2 (Figure 6). The synthetics include all fundamental spheroidal and toroidal modes to $f = 15$ mHz. Vertical dashed lines are plotted to comparing the phase delay between components. (a) Synthetics for a model with $P$ velocity anisotropy ($B = 0.06$ and $C = 0.00$). (b) Synthetics for a model with $S$ velocity anisotropy ($E = 0.02$).

Rayleigh ($QR$) waves can be generated in long-period seismic records by lateral variations in upper mantle anisotropy. Anomalous waveforms observed at a seismic station are determined by anisotropic properties along the wave path and, in principle, can be used to study anisotropic structure anywhere between the source and receiver. For fundamental branch surface waves, Love-to-Rayleigh and Rayleigh-to-Love conversions take place progressively as a surface wave travels through lateral gradients of anisotropy. After conversion from a Love wave, the quasi-Love wave has elliptical polarization and propagates with the Rayleigh group velocity. Waveform anomalies are easy to observe for a quasi-Love wave generated far from the seismic source because its arrival time can be separated from that of $R_1$. It is not surprising that the data for which we report quasi-Love wave observations are mainly from records with epicentral distances $\Delta > 50°$. As the distance between receiver and the location of the Love-to-Rayleigh "scatterer" increases, the time separation between the Love wave and quasi-Love wave also increases. Measurement of the $QL$ arrival time, relative to the main Love wave, can therefore help us locate where anisotropic structure is. Quasi-Love wave

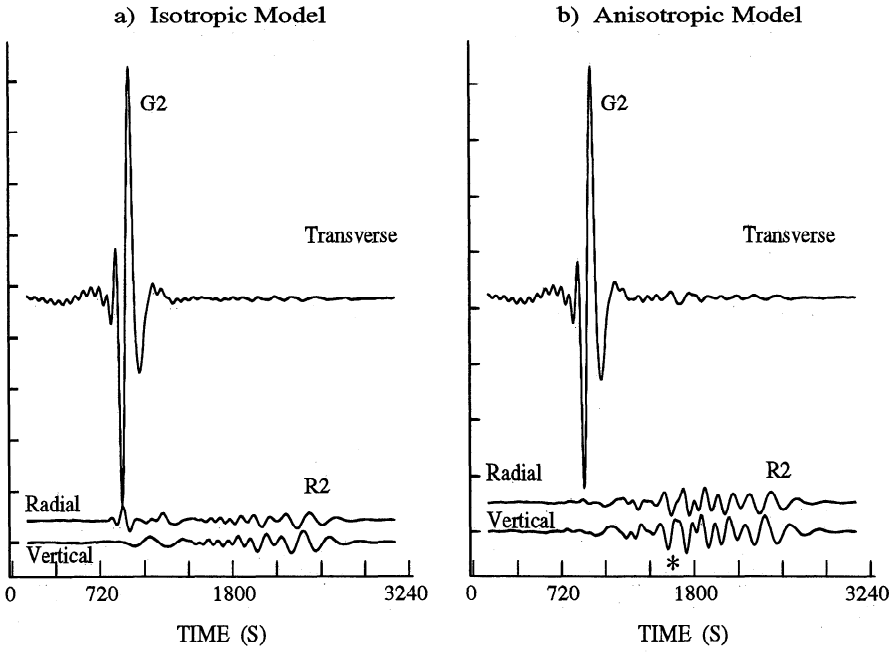


**Figure 9.** Coupled-mode synthetic seismograms for aspherical Earth models with sharp gradients midway between source and receiver. The source is located at Site 1 and receiver at Site 3 (Figure 6). The synthetics include all fundamental spheroidal and toroidal modes to $f = 15$ mHz. G2, the second wave packet of Love waves; R2, the second wave packet of Rayleigh waves. (a) Synthetics for an isotropic Earth model. (b) Synthetics for an anisotropic Earth model. The asterisk marks the $QL$ waveform anomaly associated with the anisotropic gradient.

are very sensitive to the orientation of the fast velocity axis. Strong waveform anomalies indicate the existence of anisotropic structure with a horizontal (azimuthal anisotropy) or subhorizontal symmetry axis, and with a fast velocity direction not parallel or perpendicular to the surface wave propagation path. No $QL$ wave in the data does not simply imply no anisotropy in the upper mantle. Anisotropy with a vertical symmetry axis (transverse isotropy) [*Yu and Park*, 1993] or azimuthal anisotropy with a fast direction parallel to surface wave propagation path generate weak waveform anomalies at best. Furthermore, quasi-Love waves are

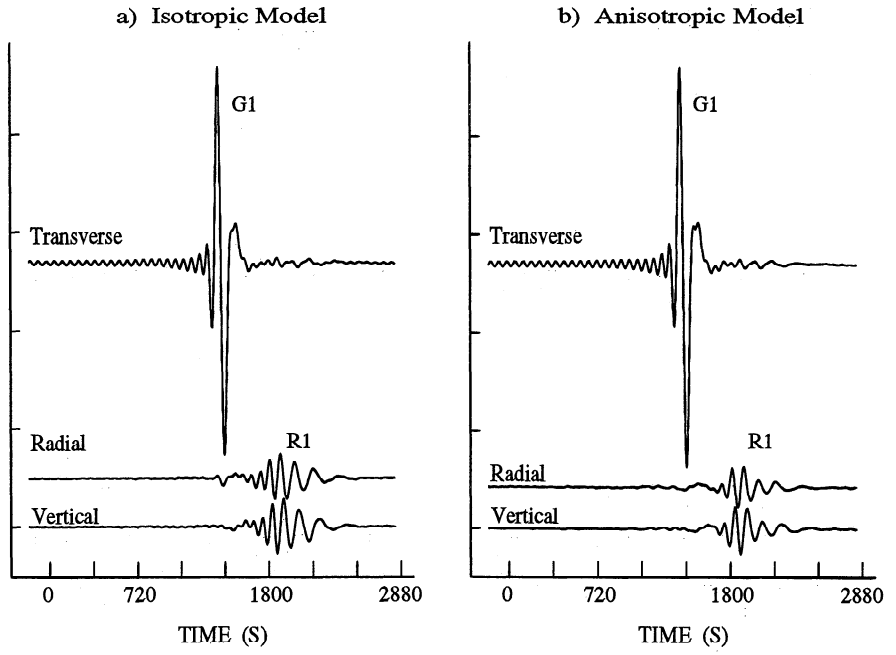


**Figure 10.** Coupled-mode synthetic seismograms for aspherical Earth models with sharp gradients close to the source (Site 2 in Figure 6) and far from the receiver (Site 3). The synthetics include all fundamental spheroidal and toroidal modes to $f = 15$ mHz. (a) Synthetics for an isotropic Earth model. (b) Synthetics for an anisotropic Earth model.

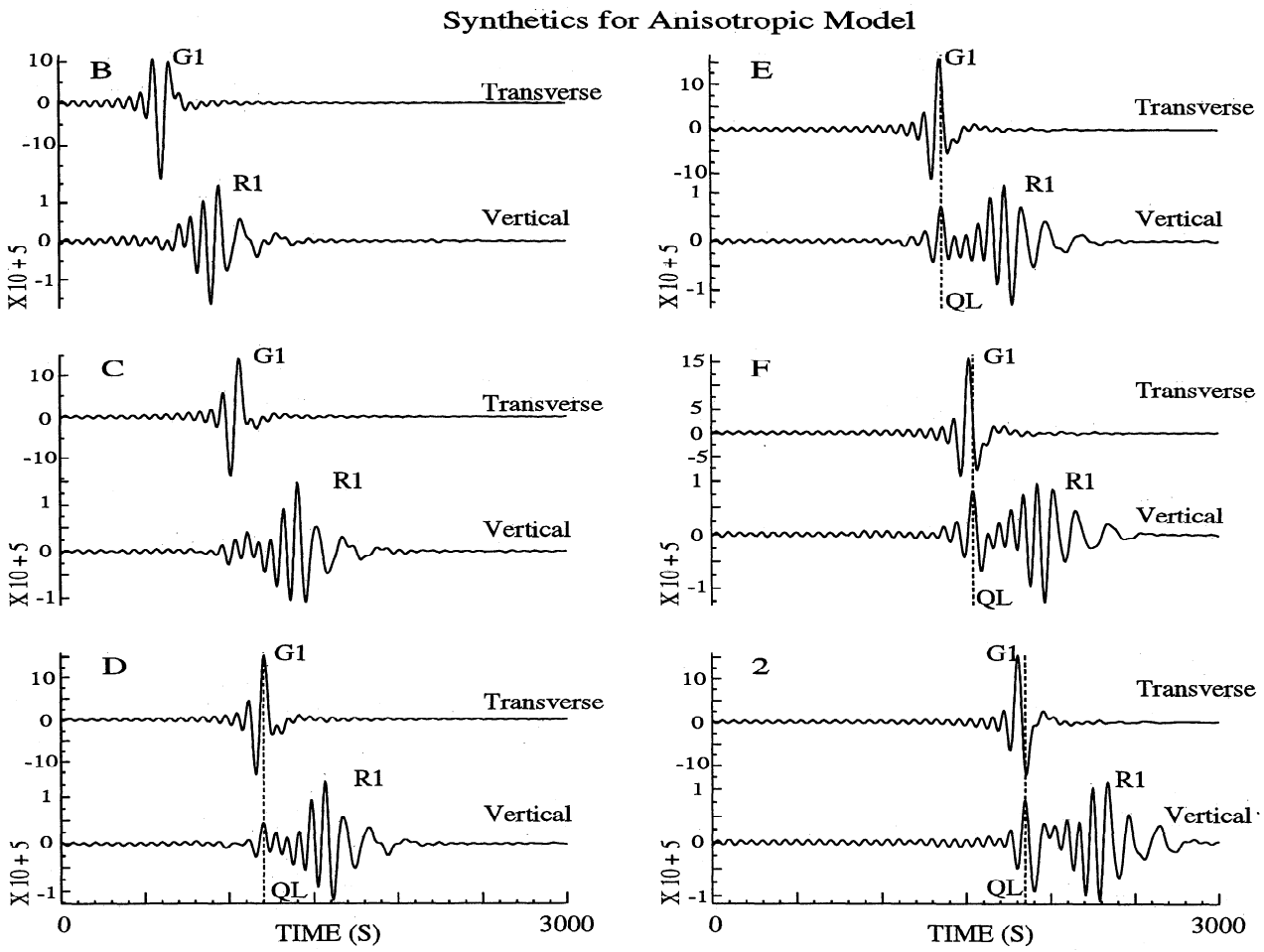


**Figure 11.** Vertical and transverse component synthetic seismograms for an anisotropic Earth model. The amplitude of the vertical component has been magnified for easier visual comparison. The synthetics include all fundamental spheroidal and toroidal modes to $f = 15$ mHz. For a fixed source at Site 1, the synthetics are calculated for receiver positions B, C, D, E, F and 2 along a single great circle path (Figure 6). The distance between the receiver and the anisotropic lateral gradient increases as the receiver moves from D to 2.

frequency-dependent. Smoother/rougher structure generates longer/shorter-period fundamental branch waveform anomalies [*Park and Yu,* 1992; *Yu and Park,* 1993; *Park,* 1993]. Strong or weak $QL$ energy may appear in the same record, but within different frequency bands. Therefore our conclusions regarding strong or weak quasi-Love waves in the data should be taken in the context of the frequency band discussed.

**Other possible causes of quasi-Love waves.** All major features of quasi-Love waves in the data can be easily replicated by simple anisotropic Earth models. However, we must consider alternative explanations. Theoretical modeling shows that Love-Rayleigh interaction due to the Earth's rotation and ellipticity, and lateral variations, even a sharp jump, in isotropic seismic velocities are either too weak to explain the anomalies, or, in the case of rotation, induce Rayleigh-Love interaction in the wrong frequency band. Strong path-dependence among $QL$ observations argues against earthquake source complexity as a responsible factor. Many events show both strong and weak quasi-Love waves at different seismic stations [e.g., *Park and Yu,* 1993]. Neither can the waveform anomalies presented above be explained by higher-mode surface waves. Higher-mode surface waves generated by a shallow, strike-slip events are usually very weak at frequencies $f \leq 15$ mHz, relative to fundamental surface waves, and arrive prior to, instead of after, the Love wave (see Figure 1). As a practical matter, fundamental mode Rayleigh-Love waveform anomalies are more difficult to identify visually if the overtone surface waves are well excited. This difficulty worsens at frequencies $f > 15$mHz, as the higher modes and the quasi-Love wave tend to arrive in similar time windows. That is why we report here the observations only for shallow, strike-slip events, even though quasi-Love waves will exist even if strong overtone surface waves are present.

Although the $QL$ wave is observed in several tectonic settings in the Pacific Ocean region, strong waveform anomalies are most prevalent for propagation paths subparallel to subduction zones, such as records at SNZO and INU for events in California. It is therefore impor-

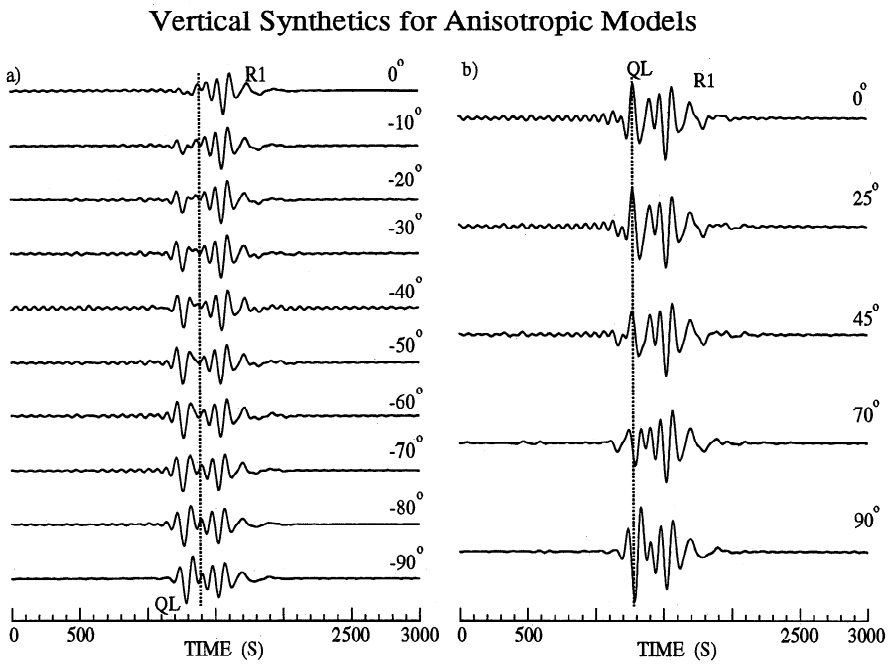


**Figure 12.** Vertical component synthetic seismograms for anisotropic Earth models. The synthetics include all fundamental spheroidal and toroidal modes to $f = 15$ mHz. Vertical dashed lines are plotted for comparing the relative arrival times of signals. (a) Synthetics for a single anisotropic Earth model (Figure 6), but for paths with different back-azimuth. The epicentral distance is fixed for all the paths. The back-azimuth changes from 0° for an event at Site 4 to $-90°$ for an event at Site A. (b) Synthetics for a fixed source-receiver pair, but for anisotropic Earth models with varying orientation of the fast $P$ wave velocity direction. The fast axis of anisotropic structure (Figure 6) rotates from the south ($\xi = 0°$) to the east ($\xi = 90°$).

tant to investigate whether dipping slab structure and the topography of the Earth, such as the deep trench above a subducting slab, could generate mixed-type coupling that is strong enough to explain the anomalies in the data. Finite difference modeling of short-period surface waves [*McLaughlin et al.*, 1992] in a trench geometry found important coupling effects. At long periods ($f \leq 15$ mHz), however, *Park and Yu* [1993] found weak mixed-type coupling in synthetics for an Earth model with 10-km peak-to-peak perturbation in the seafloor. We have also calculated synthetic seismograms for an isotropic Earth model with a 45° dipping slab. Even if the $S$ wave velocity perturbation within the slab is 6% higher than the surrounding region, we cannot generate significant quasi-Love waveform anomalies with $f < 15$ mHz.

## Observations and Discussion

To find evidence for upper mantle anisotropy beneath the Pacific Ocean, we have analyzed digital three-component long-period seismograms recorded at stations from the Incorporated Research Institutions for Seismology/U.S. Geological Survey (IRIS/USGS), International Deployment of Accelerometers (IRIS/IDA), Chinese Digital Seismic Network (CDSN) and Geoscope networks. For simplicity in interpretation, long-period seismic records are low-passed at corner frequency $f_C = 15$ or 20 mHz. Surface waves in this frequency band sample principally the mantle. We choose seismic records for large, shallow, predominantly strike-slip events since long-period surface waves for these events are relatively simple and are dominated by fundamental Rayleigh and Love motions. Surface wave refraction and Rayleigh-Love coupling are easiest to observe for the stations near the Love and Rayleigh radiation nodes. Quasi-Rayleigh ($QR$) waves can be observed near the Love radiation node but are often obscured by Love wave coda, the higher noise level on horizontal components, difficulties in distinguishing a refracted Rayleigh wave on the transverse component, and, sometimes, incorrect rotation of horizontal records into transverse and radial components. Quasi-Love waves can be observed near the Rayleigh radiation node, and precede the Rayleigh wave on the more quiet vertical component. Thus most of our data observations are $QL$ waves from seismic stations with azimuth $\lesssim 15°$ from the Rayleigh radiation node.

### Observations in the Northwest Pacific Ocean

Observations of quasi-Love waves in the northwest Pacific Ocean region, summarized in Figure 13, depend strongly on the propagation path. Strongly coupled $QL$ waveforms are observed for paths in the northwest Pacific Ocean basin or immediately east of the Marianas-Izu-Bonin subduction zone. Figure 14a shows the LP-

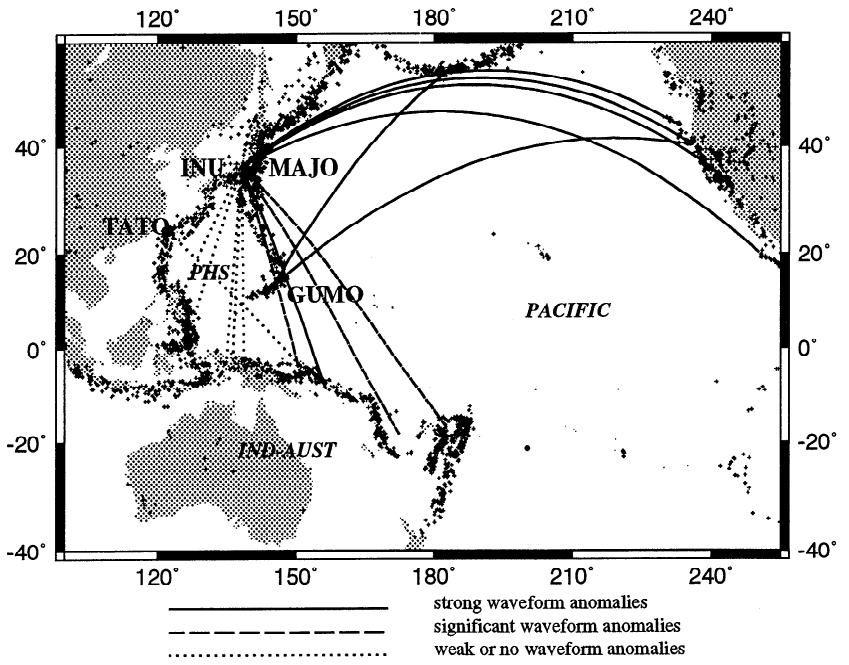


**Figure 13.** Source-receiver paths for quasi-Love observations in the northwest Pacific Ocean region. Solid lines show paths with very strong $QL$ waveform anomalies. Dashed lines are for paths with significant $QL$ waveform anomalies. Dotted lines are for paths with no or very weak waveform anomalies. The locations of seismic stations INU, MAJO, TATO and GUMO are marked. Also plotted are 1988-1991 epicenters from the NEIC daily bulletins. These earthquakes outline the plate boundaries.

channel seismic record at station MAJO (Matsushiro, Japan) for the May 9, 1983, Revilla Gigedo Islands event (NEIC epicenter 19.98°N, 109.45°W, $d = 10$ km). The source-receiver great circle crosses the north Pacific Ocean and intersects the Japan Trench near the station. Note the $QL$ wave on the vertical component record that arrives slightly behind $G_1$ on the transverse component record. Similar waveforms are observed at station MAJO and INU for many large earthquakes along the coast of California (e.g., Figure 5b). In contrast, waveform anomalies are absent from surface waves crossing the Philippine Sea. Figure 14b shows the low-passed

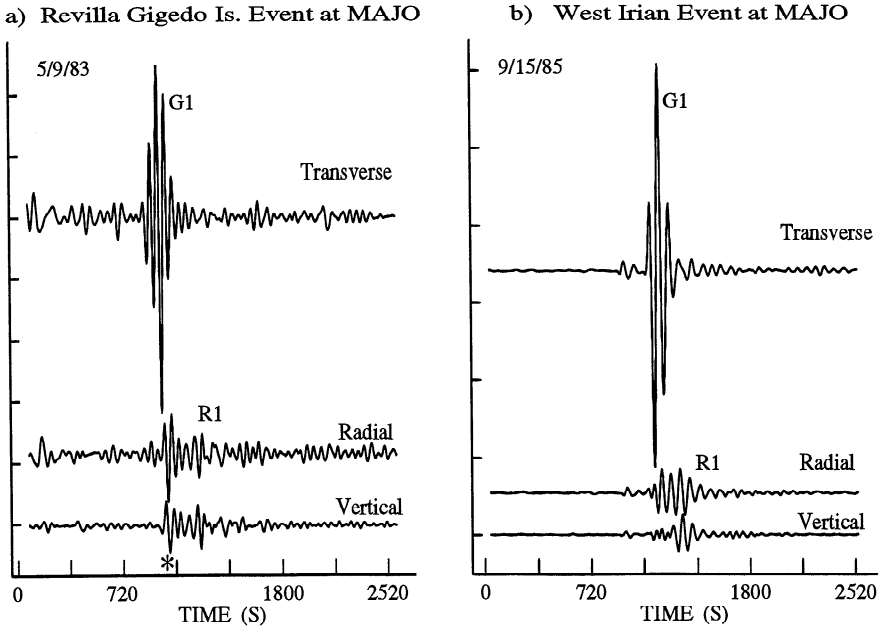


**Figure 14.** (a) LP-channel motion recorded at station MAJO (Matsushiro, Japan) for the May 9, 1983, Revilla Gigedo Islands event ($M_S = 6.2$). The asterisk marks the waveform anomaly. (b) LP-channel motion recorded at station MAJO for the September 24, 1983, West Irian event ($M_S = 6.3$). For the both events, the data are low-passed at 15 mHz.

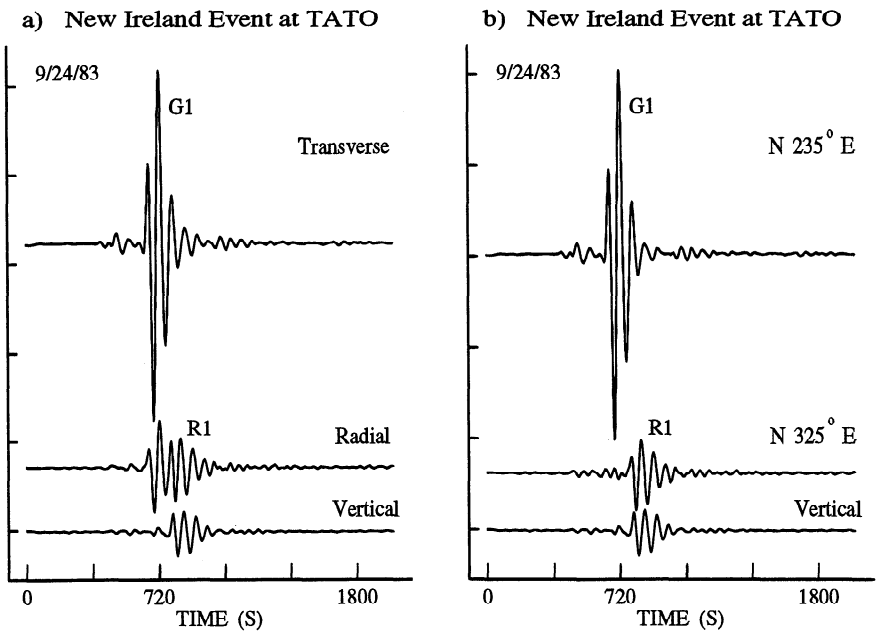


**Figure 15.** LP-channel data recorded at station TATO (Taipei, Taiwan) for the September 24, 1983, New Ireland event ($M_S$ = 6.0, NEIC epicenter 3.79°S, 151.15°E, $d$ = 33 km). The data are low-passed at 15 mHz. (a) Seismic motion after rotating the horizontal data onto the radial (N310°E) and transverse directions. (b) Seismic motion after rotating the horizontal components to the azimuth N325°E, 15° from the great circle path.

MAJO record for the September 15, 1985, West Irian event (NEIC epicenter 4.17°S, 136.23°E, $d$ = 10 km). No significant waveform anomaly appears on the vertical component before $R_1$ and after $G_1$. Some energy appears on the radial component record with the arrival of Love wave packet $G_1$ and is due to refraction. Figure 15a demonstrates the refraction effect for another record at TATO (Taipei, Taiwan) for an event in the New Ireland region. Note that after rotating the horizontal components to the azimuth N325°E, 15° from the great circle path, the refraction anomaly disappears on the "radial" component (Figure 15b). There is no quasi-Love wave in this record.

Quasi-Love precursors in the northwest Pacific Ocean show a good correlation between waveform anomalies and plate tectonics. Strong quasi-Love waves shown in the data for the surface waves propagating on the downgoing (Pacific plate) side of the Marianas-Izu-Bonin plate boundary argue strongly for laterally varying anisotropy near the plate boundary (Figure 13). In contrast, surface waves on the other side of plate boundary (in the Philippine Sea) exhibit weak or no quasi-Love waves. Similar behavior was reported from Japanese broadband observations of 1989 Macquarie Ridge event by *Kato and Hirahara* [1992], who describe what appear to be quasi-Rayleigh waveforms. Several seismic records at MAJO, INU and TATO for the strike-slip events from Mindanao to the Vanuatu Islands show a good azimuth coverage in the Philippine Sea (Figure 13). Therefore it seems unlikely that all the paths are parallel to the fast direction if azimuthal anisotropy exists beneath the Philippine Sea. The results from the global inversion of 200-s Rayleigh wave phase velocity [*Tanimoto and Anderson,* 1984] also show weak azimuthal anisotropy in the same region. Fine details of global models are often poorly constrained, but these correlations encourage further investigation.

Transversely isotropic or fully isotropic structure would explain the weakness of quasi-Love waves in the Philippine Sea region. Transverse isotropy would be consistent with the symmetry axis of upper mantle peridotites aligned with nearly vertical mantle return flow. This is consistent with the upper mantle kinematic flow model calculated by *Hager and O'Connell* [1979], which predicted near-vertical mantle flow under the Philippine Sea. Another explanation is the disruption of peridotite lattice-preferred orientation (LPO) by processes related to island arc volcanism behind the Marianas-Izu-Bonin subduction zone. For instance, water released by the slab would lower the melting temperature in the overlying wedge, lower its seismic velocity, and would also inhibit the development of LPO anisotropy [*Karato et al.,* 1986].

## Observations in the Central Pacific Ocean

Quasi-Love waves recorded at station KIP and HON suggest the presence of azimuthal anisotropy in the central Pacific Ocean near Hawaii (Figure 16). Eight percent $P$ wave velocity anisotropy with a nearly east-west fast direction was inferred near Hawaii from early studies of travel time residuals [e.g., *Morris et al.,* 1969]. Strong $SKS$ wave splitting (1.5 s) has been reported at KIP by *Vinnik et al.* [1992], but equivocal results were reported at other Hawaii stations by *Kuo and*

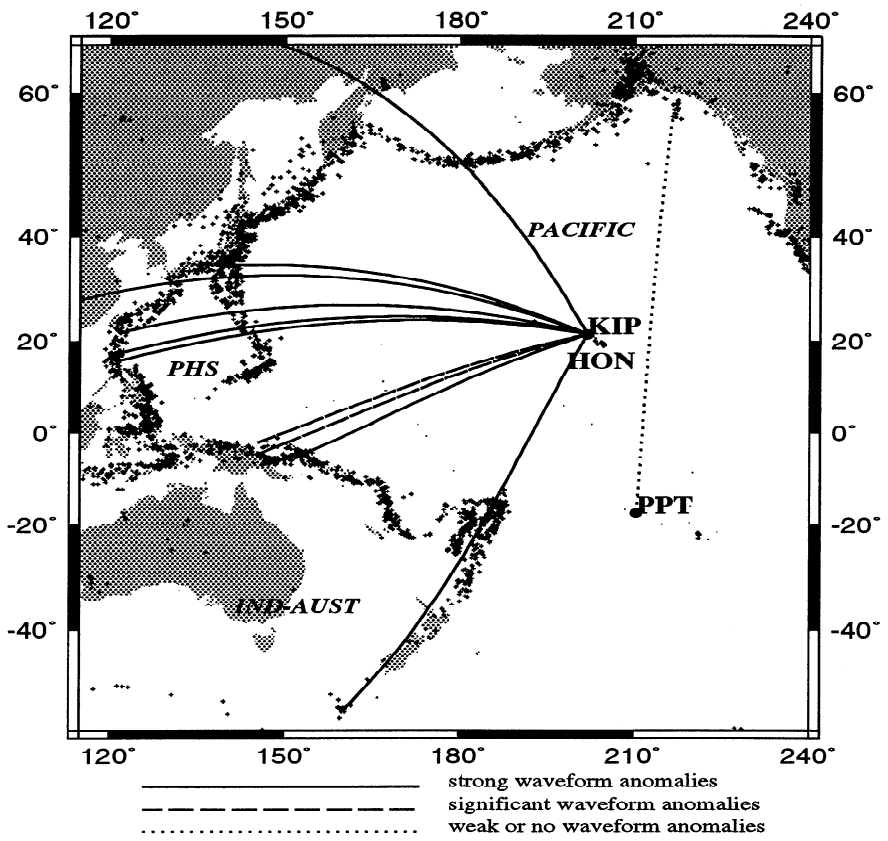


**Figure 16.** Same as Figure 13, showing source-receiver paths for quasi-Love observations in the central Pacific Ocean region. The locations of seismic stations KIP, HON and PPT are marked.

*Forsyth* [1992]. Our observation of $QL$ waves at KIP indicates the existence of strong anisotropic gradients near Hawaii. The delay of the quasi-Love wave, relative to Love, on the KIP record from the June 20, 1992, Western Iran event suggests an anisotropic gradient $\approx$ 3000 km NW of Hawaii. If due to variations in fossil anisotropy within the Pacific plate, this is consistent with the spreading history of the northwestern Pacific [*Nishimura and Forsyth,* 1988], determined from magnetic anomalies that predate the Cretaceous long normal. $QL$ waves on paths from the west and southwest suggest Love-to-Rayleigh conversion also occurs close to KIP (Figure 5a). Reheating of lithospheric material or asthenospheric flow beneath the Hawaiian hotspot may be responsible. The observations at KIP for the July 16, 1990, Philippine event (Figure 4b) favor a model with gradients in $P$ wave anisotropy ($B$) only, because no significant Love wave refraction is evident in the records, unless the Love refractions induced by $C$, $D$ and $E$ structure cancel.

In the central Pacific Ocean, strongly frequency-dependent $QL$ anomalies are observed at Geoscope station PPT (Papeete, Tahiti). Figure 17 shows VH-channel seismic record at PPT for the March 6, 1988, $M_S = 7.4$ earthquake in the Gulf of Alaska, a strike-slip event (NEIC epicenter 57.37°N, 143.53°W, $d = 15$ km). In this case long-period surface waves propagate along a purely oceanic path, far from plate boundaries. For the record low-passed at corner frequency 8 mHz (Figure 17a), the vertical component record shows some $f \lesssim 4$ mHz energy before Rayleigh wave packet $R_1$, consistent with Coriolis coupling associated with Earth rotation [*Park,* 1986]. The strong energy on the radial component, coeval with $G_1$, is due to Love wave refraction. Mixed-type coupling due to aspherical Earth structure is very weak in the frequency band of 4-8 mHz. However, band passing to 8-15 mHz shows a significant waveform anomaly likely associated with Rayleigh-Love coupling (Figure 17b). This behavior differs from $QL$ waves seen at station KIP (Figure 4b), where strong waveform anomalies are observed in the frequency band of 4-8 mHz.

How do we reconcile the weak long-period $QL$ wave on the Alaska-PPT path with the observations from marine refraction experiments [*Christensen,* 1984] that show strong azimuthal anisotropy along this source-receiver path? The weak quasi-Love anomaly with $f < 8$ mHz could be attributed to anisotropy at shallow depth under the open ocean basin, since the long-period surface waves with $f < 8$ mHz sample more deeply in the mantle. However, coupled-mode synthetics suggest that the long-period content of a quasi-Love wave is only weakly sensitive to the depth of anisotropic structure, at least in the top 300 km of the mantle. Therefore it is very difficult to model the PPT waveform anomaly with a sharp lateral gradient model. However, the fre-

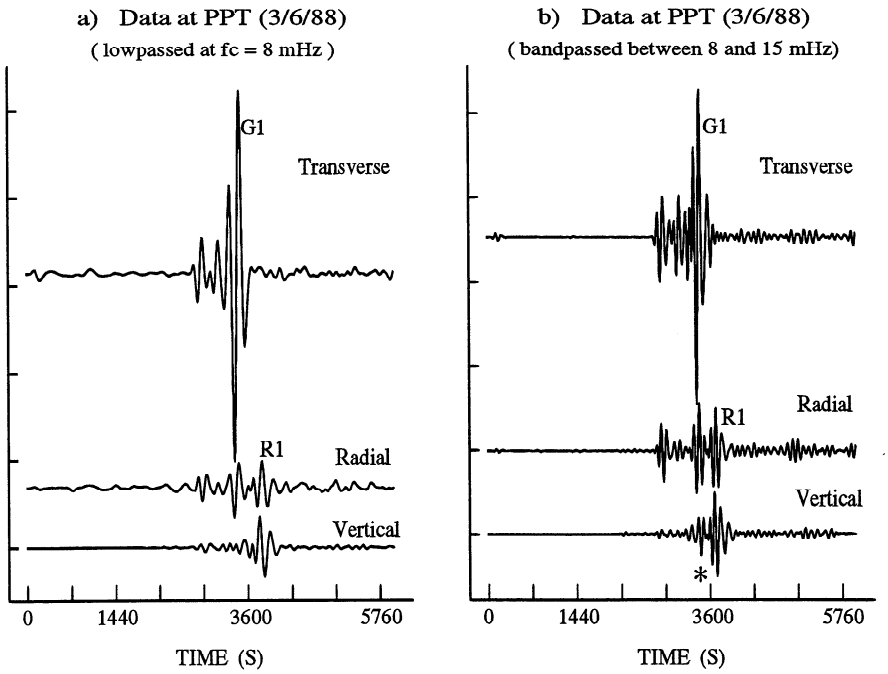


**Figure 17.** VH-channel data recorded at Geoscope station PPT (Papeete, Tahiti) for the March 6, 1988, Gulf of Alaska event ($M_S = 7.6$). (a) Seismic motion after low-passing at 8 mHz. (b) Seismic motion after bandpassing between 8 and 15 mHz. The asterisk marks the $QL$ waveform anomaly.

quency content of the $QL$ wave is also sensitive to the lateral wavelength of anisotropic upper mantle structure [*Park and Yu,* 1992; *Yu and Park,* 1993]. A smooth anisotropic model with the wavelength of a spherical harmonic with angular degree $s \approx 16$ generates significant waveform anomalies in the 8-15 mHz band pass, but very weak anomalies for $f < 8$ mHz. Therefore the record at PPT may indicate that the anisotropic structure between source and receiver has a special wavelength. The wavelength for $s \approx 16$ is $\sim 2400$ km, approximately equal to twice the distance between major fracture zones in the north central Pacific Ocean. These fracture zones trend east-west and are regularly spaced in this part of the Pacific plate. One possible mechanism would be that different ridge segments in the ancient Pacific, bounded by major transform faults, acquired different amounts of anisotropy as the lithosphere formed. Another possibility is that LPO anisotropy developed near transform faults differs from that developed in the middle of ridge segments. The dominant wavelength of this latter mechanism, however, would be half that necessary to model the PPT waveform.

## Observations in the Southwest Pacific Ocean

Strong quasi-Love waves are observed at New Zealand station SNZO from the paths with a northeast azimuth (Figure 18). Most of these propagation paths intersect the Tonga-Kermadec subduction zone near the receiver. A significant quasi-Love waveform anomaly is also observed for the path from the November 4, 1992, Balleny Island event to station RAR [*Park and Yu,* 1993], suggesting that Love-to-Rayleigh conversion is not restricted to the subduction zone itself. In contrast, no waveform anomalies are observed for the surface waves propagating along the SE Indian Ridge and southwest of New Zealand.

**Modeling quasi-Love wave waveforms at SNZO.** Can the quasi-Love waveform anomalies in the SW Pacific Ocean be modeled using simple anisotropic models? The answer is yes, at least for selected cases. As an example, we performed a waveform fitting experiment using long-period SNZO seismic records. The $QL$ waves in the data arrive closely behind $G_1$ and are distinct from the Rayleigh wave packets (Figure 2). We hypothesize that these $QL$ waves were generated by strong lateral gradients in anisotropic structure near the receiver, possibly in front of the Tonga-Kermadec subduction zone. To better understand the sources of the observed anomalies, we take the following steps: We rotated the sharp boundary in our simple model (Figure 6) to coincide with the subduction zone. We adjusted the boundary's strike and distance from the Tonga-Kermadec subduction zone by varying the source and receiver locations, while holding the epicentral distance fixed. We specified 6% peak-to-peak $P$ wave velocity anisotropy in the top 200 km of upper mantle. We calculated synthetic seismograms from sums of coupled free oscillations for a suite of models by varying the symmetry axis in the $\theta\phi$ tangent plane on either side of the sharp boundaries at $\pm 45°$ latitude, comparing synthetic quasi-Love waves to those observed in the data.

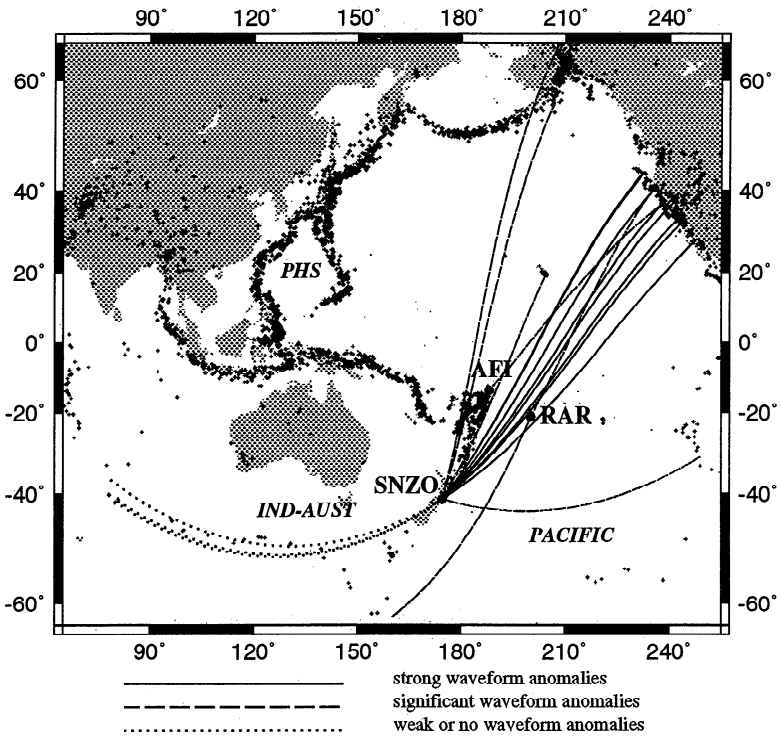


**Figure 18.** Same as Figure 13, showing source-receiver paths for quasi-Love observations in the southwest Pacific Ocean region. The locations of seismic stations SNZO, AFI and RAR are marked.

Quasi-Love waves in the data are significantly stronger than those generated by the anisotropic model with $B \neq 0$ in only the polar caps. To boost the $QL$ amplitude, we added 6% $P$ wave velocity anisotropy in the equatorial belt $-45° < \theta < 45°$, with fast direction perpendicular to the boundary. This changes the sharp boundary to anisotropic-anisotropic, so that the lateral gradient involves a 90° rotation of the fast $P$ wave direction. The modified model generates $QL$ waves whose amplitude, relative to the main Love wave, is comparable with data. Figure 19 shows the comparison between the data and synthetic waveform calculated from the best fit model of Figure 20. Both Love and quasi-Love waves in all the records are fit well. However, the Rayleigh wave packets are poorly modeled. Because the observations at SNZO come from the Rayleigh radiation node, the Rayleigh wave packets may suffer off-path refraction from lateral structure more complex than our simple sharp gradient.

It should be pointed out that more than one model can fit the SNZO data. The sensitivity analysis of the waveform to the symmetry axis azimuth (Figure 12) suggests an uncertainty of roughly ±15°. The effect of azimuth would trade off with the amplitude of the $B$ coefficient. A curved lateral gradient could focus the quasi-Love waveform to increase its amplitude. At least for the long-period portion of the observed $QL$ waves, the sharp boundary in Figure 20 could be replaced by a transition zone of as much as 1000 km, in which the fast $P$ direction changes smoothly from perpendicular to parallel to the Tonga-Kermadec trench. As indicated by *Park* [1993], the anisotropic parameters $C$ and $E$ in (1) are more efficient than $B$ in generating mixed-type coupling. Marine refraction data offer poor constraints on $C$, the $4\eta$ term in $P$ wave velocity, because a good azimuth coverage is difficult to achieve; nevertheless, most estimates restrict $C < 0.01$. $S$ wave velocity anisotropy in the upper mantle is expected to be smaller than $P$ wave velocity [*Peselnick and Nicolas,* 1978; *Christensen,* 1984; *Anderson,* 1989; *Mainprice and Silver,* 1993], perhaps in the range of 1–4%. An anisotropic model with 1% $4\eta$ term $P$ wave velocity anisotropy ($C = 0.01$) could generate $QL$ waves of sufficient amplitude in the long-period seismic records, as well as significant Love wave refractions. A 2% $S$ anisotropy ($E = 0.02$) in the asthenosphere (100-300 km) with the lateral variations of our shallower best fit $P$ anisotropy model (Figure 20) can also fit the data reasonably well. However, the combination of shallow $P$ and $S$ anisotropy actually diminishes the $QL$ waveforms somewhat. At face value, the observations at SNZO favor a model with gradients in $S$ wave anisotropy because significant Love wave refractions are evident in the records. However, because isotropic $S$ wave lateral structure can also generate Love wave refractions, there is a trade-off between isotropic and anisotropic parameters, when both quasi-Love waves and Love wave refractions are considered.

**Upper mantle anisotropy near the Tonga-Kermadec Trench.** The delay of a quasi-Love wave, relative

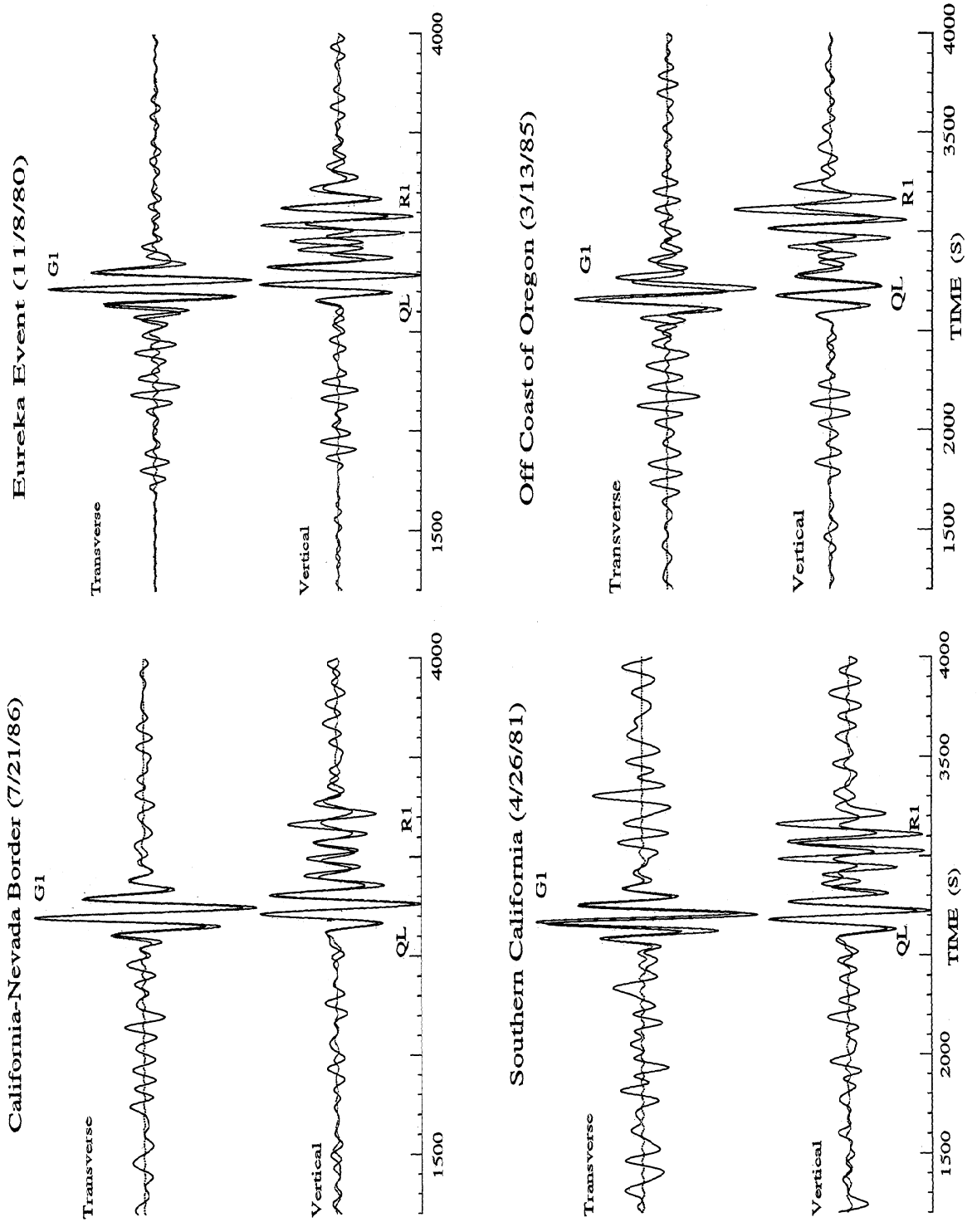


**Figure 19.** Comparison between the data recorded at SNZO and fundamental mode synthetic seismograms calculated from a best fit anisotropic Earth model obtained by trial-and-error forward modeling. Data and synthetics are bandpassed between 6 and 13 mHz. The solid lines show the data. Dashed lines show the synthetics.

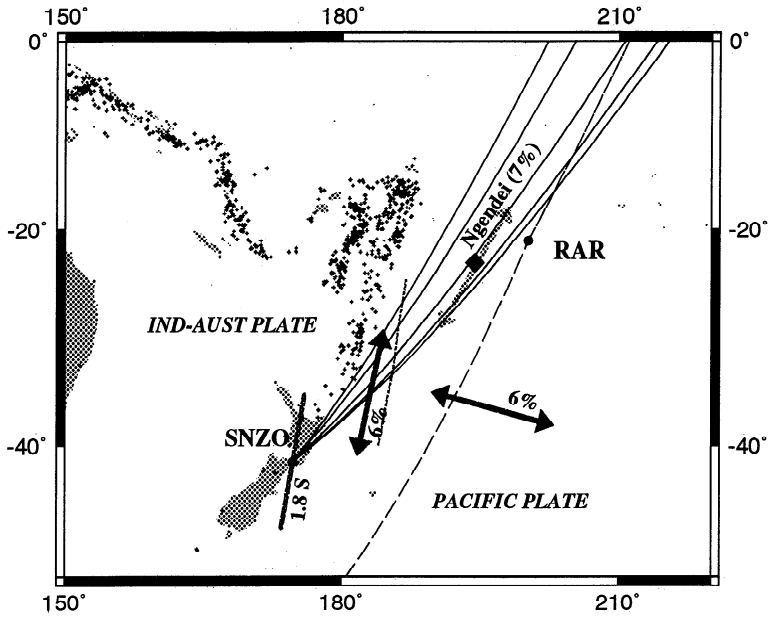


**Figure 20.** An anisotropic Earth model which can fit the quasi-Love waves observed at station SNZO. The line in front of the Tonga-Kermadec subduction zone indicates the position of a strong anisotropic gradient, caused by a sharp rotation in the orientation of fast $P$ wave velocity. The solid arrows show the fast $P$ wave velocity direction on either side of this transition. The solid and dashed lines show the great circle paths for which significant quasi-Love waveform anomalies are observed in the data. Also plotted are 1988-1991 epicenters from the NEIC daily bulletins, which outline the plate boundary between the Pacific plate and the Indo-Australian plate. The site and inferred $P$ anisotropy of the Ngendei seismic refraction experiment [*Shearer and Orcutt,* 1986] is shown for comparison. Also shown is the result from $SKS$ splitting analysis at SNZO [*Vinnik et. al.,* 1992]. The symbol at SNZO indicates the fast polarization direction, and the $SKS$ delay time (1.8 s) is marked.

to the Love wave, is sensitive to the distance from the anisotropy gradient and can help us determine where the converted wave was generated. Forward modeling of quasi-Love wave "arrival time", relative to the main Love wave, and of the long-period quasi-Love waveform on those records suggests that the Love-to-Rayleigh conversion takes place about 1200-1600 km from station SNZO. The strong Love-to-Rayleigh conversion near station SNZO can be modeled well by a sharp boundary with strike N7.6°E in front of the Tonga-Kermadec subduction zone. The boundary can be modeled as a sharp change in fast $P$ wave (or $S$) velocity direction near the subduction zone. The fast direction rotates from nearly perpendicular to the subduction zone far from the trench (parallel to south Pacific fracture zones) to N7.6°E near the trench (and parallel to it). Six percent $P$ wave anisotropy ($B = 0.06$, $C = E = 0.0$) is specified in our best fit model, obtained with trial-and-error forward modeling. This level of anisotropy is consistent with the observations from peridotite samples and marine refraction experiments [e.g., *Peselnick and Nicolas,* 1978; *Christensen,* 1984; *Shearer and Orcutt,* 1986; *Mainprice and Silver,* 1993]. The presence of a strong anisotropic gradient in front of the subduction zone is also supported by strong $QL$ waves, observed at station RAR, for the November 4, 1992 Balleny Island event [*Park and Yu,* 1993]. For this record, the surface wave propagates in the New Zealand shelf without crossing a plate boundary. For two large earthquakes (April 26, 1992) in northern California, surface waves recorded at station RAR and SNZO have a similar propagation path in the east and central Pacific Ocean. However, station RAR is in front of the sharp boundary inferred from our waveform fitting (Figure 20) and station SNZO is behind the boundary. The quasi-Love waves observed at SNZO are much larger than those observed at RAR (Figure 21), supporting our inference that there is a strong anisotropic gradient between RAR and SNZO. The absence of quasi-Love anomalies at SNZO from events on the southeast Indian Ridge does not require the absence of upper mantle anisotropy along the paths. Anisotropy with weak lateral gradients or with a fast axis parallel to wave propagation path generates weak anomalies, and cannot be ruled out. The laterally varying anisotropy near the Tonga-Kermadec Trench can be attributed to the following mechanisms:

**Variations in the asthenospheric flow:** Azimuthal anisotropy in the asthenosphere may differ from fossil anisotropy in the lithosphere, as it is associated with present-day plate motion or related mantle flow. Based on the study of seismicity and focal mechanisms in the Tonga Islands region, *Giardini and Woodhouse* [1986] proposed that the Pacific plate, the Australian plate and shallow slab at the Tonga Trench are moving north-

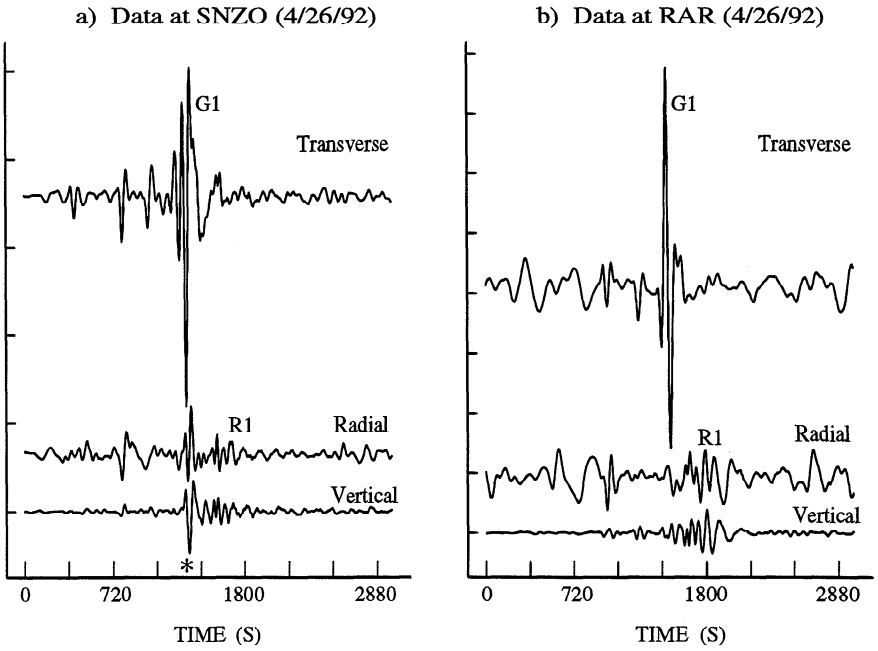


**Figure 21.** LH-channel motions recorded for one of the April 26, 1992, events near the Northern California Coast ($M_S = 6.7$, NEIC epicenter 40.38°N, 124.57°W, $d = 22$ km). The data are low-passed at 15 mHz. (a) Seismic motion at station SNZO. The asterisk marks the $QL$ waveform anomaly. (b) Seismic motion at station RAR (Rarotonga Island), where the $QL$ anomaly is less pronounced.

ward with respect to the surrounding mantle at ~ 5 cm/yr, a speed comparable with the convergence velocity. *Fischer et al.* [1991] also inferred unusual lateral strains in the Tonga subduction zone from seismic source mechanisms and slab structure. The strong horizontal shear flow in the mantle should produce lattice-preferred orientation (LPO) in the rock and thus give rise to a bulk anisotropy of mantle materials, with the fast axis aligned with the principal extension axis of the strain ellipsoid or the direction of mantle flow [*McKenzie,* 1979; *Christensen,* 1984; *Nicolas and Christensen,* 1987; *Ribe,* 1989a, b; *Ribe and Yu,* 1991]. Therefore azimuthal anisotropy with a roughly north-south symmetry axis would be predicted at 100-400 km depth in the Tonga subduction zone, its extension eastward determined by the ambient mantle viscosity. This is consistent with our observations in the southwest Pacific Ocean. This mechanism would also complement the inference of trench-parallel mantle flow by *Russo and Silver* [1994] beneath South American subduction zones.

**Variations in the fossil spreading direction:** The fast direction of $P$ wave velocity in an oceanic plate is expected to be parallel to the fossil spreading direction [e.g., *Ribe,* 1989b]. There are significant differences in the direction of absolute plate motion and fossil seafloor spreading in the southwest Pacific Ocean [*Nishimura and Forsyth,* 1988]. Therefore the inferred sharp rotation of the fast axis in our best fit $P$ anisotropy model could reflect variations in fossil spreading direction in older portions of the Pacific plate. Previous $P$ wave travel time studies suggested that the uppermost mantle is anisotropic in this area. Travel times from a large number of regional events reveal a variation of $P$ velocity with azimuth [*Galea,* 1993], suggesting 7.7% $P$ wave velocity anisotropy in the mantle lid (depths $\lesssim$50 km) in the Pacific northeast of New Zealand. Only weak $P$ anisotropy was inferred beneath the lid. Since this portion of the Pacific plate was formed during the Cretaceous long normal polarity interval, there are no magnetic anomalies to check the fossil spreading direction independently. However, the Ngendei marine refraction experiment [*Shearer and Orcutt,* 1986] supports the presence of sub-Moho anisotropy, at least at one point west of RAR (Figure 20). Seven percent $P$ wave anisotropy with a N30°E fast direction is inferred from the Ngendei experiment, roughly consistent with *Galea* [1993]. *Montagner and Tanimoto* [1990, 1991] inferred global maps of azimuthal anisotropy from the tomographic inversion of long-period surface wave phase velocities. The global studies parameterize their models in low-degree spherical harmonics, and so would smooth out the sharper gradients inferred by our analysis. Even so, if we relate phase velocity to shear velocity only, their global models suggest that the fast axis of shallow (100 km) shear wave anisotropy ($\lesssim$2%) rotates from roughly WNW-ESE in the southern Pacific to N-S near the Tonga trench and New Zealand, consistent with our interpretation. Deeper in the upper mantle, the model of *Montagner and Tanimoto* [1991] does not exhibit a rotation of the symmetry axis near Tonga-Kermadec.

Two factors, however, argue against changes in fossil spreading rates as the cause of the observed SNZO waveform anomalies. First, the regional anisotropic

gradient responsible for the SNZO waveform anomalies is fairly close to station SNZO, but the NE-SW $P$ anisotropy in the lid is inferred to extend as far as RAR [*Shearer and Orcutt,* 1986]. Moreover, there is a significant difference between the symmetry axis inferred by us and that inferred from the regional travel time observations. In front of Tonga-Kermadec trench, *Galea* [1993] inferred a fast $P$ velocity direction of N62°E. Our synthetic seismogram experiments (section 3) predict that weak quasi-Love waves would be observed at SNZO because the paths from California are nearly parallel to this symmetry axis.

**Disturbance by a hotspot:** The third mechanism we consider is motivated by the proximity of the Louisville Ridge to the sharp gradient inferred by our $QL$ waveform fitting exercise. The Louisville "Ridge" is a line of seamounts likely caused by a hotspot, as its gravity signature extends southeast, paralleling a south Pacific fracture zone for several hundred kilometers [*Sandwell and Smith,* 1992]. Therefore we cannot rule out the possibility that the reheating of lithospheric material beneath the hotspot could be a contributing factor to the lateral gradient in the anisotropic upper mantle. On the basis of three-dimensional geodynamic modeling, however, *Ribe and Christensen* [1994] argue that reheating associated with a typical mantle plume will not penetrate the mantle lid to a significant extent. Perturbed flow in their models is largely restricted to the asthenosphere, where a "stagnation streamline" separates preexisting mantle flow from plume spreading. Shear along this streamline could give rise to lateral gradients in anisotropy. Such gradients would likely differ from the geometry described in Figure 20, but this geometry may not be uniquely determined by the SNZO data.

**Lithospheric compression:** It is also possible that the fast axis of lithospheric anisotropy changes its orientation near the convergent plate boundary where strong deformation is expected. *Vinnik et al.* [1992] identifies strong $SKS$ splitting at SNZO with a NE-SW symmetry axis (Figure 20), and associates this signal with compression of the New Zealand continental fragment along the Alpine fault. It is not clear that this mechanism would affect oceanic lithosphere, as it avoids collisional compression by subducting. The New Zealand continental fragment does not extend to the northeast sufficiently far to explain the timing of quasi-Love waves at SNZO.

## Conclusions

We have investigated long-period surface waves ($f <$ 15 mHz, $T \gtrsim 70$ s) that propagate in the Pacific Ocean region. Significant quasi-Love waveform anomalies, caused by fundamental Love-Rayleigh coupling, are consistently observed in the data. Lateral variation in upper mantle anisotropy is a likely explanation for those anomalies. The results from analyses of a large number seismic records suggest that a significant portion of the upper mantle beneath the Pacific Ocean is strongly anisotropic. In particular, our observations of quasi-Love waves indicate the existence of strong anisotropic gradients in the older part of Pacific Ocean basin and near Hawaii. A lack of quasi-Love generation beneath the Phillipine Sea suggests weak azimuthal anisotropy in the region. Quasi-Love waveforms observed at station SNZO can be well modeled by a strong anisotropic gradient in front of the Tonga-Kermadec subduction zone. The gradient could be attributed to flow variations in the mantle, variations in fossil spreading direction in the Pacific plate, or a combination of the two. Gradients in azimuthal anisotropy are inferred in the northwestern Pacific, associated with one or more of mechanisms of variations in asthenosphere flows, fossil spreading direction, and/or hotspot tracks. A quasi-Love wave observed on a path from Alaska to PPT is band-limited to $f > 8$ mHz, suggesting lateral variations with wavelength twice the spacing of fracture zones in the north central Pacific.

The details of upper mantle anisotropy, such as its amplitude and orientation, its depth dependence, are not yet constrained well from our forward modeling waveform analysis. The difficulties arise from several aspects. Our modeling for quasi-Love waves in an aspherical Earth model are limited to highly simplified models and low frequencies ($f < 20$ mHz). The restriction to the stations near Rayleigh wave nodes greatly reduces the number of robust $QL$ observations. More observations are needed for further study, and this will entail the identification of Love-Rayleigh coupling effects for a wider variety of source azimuths and mechanisms.

**Acknowledgments.** Karen Fischer, Ken Creager, Art Lerner-Lam, and Neil Ribe made useful comments on this research. Comments from the reviewers and Associate Editor helped improve the paper's exposition. Data for this project were obtained from several broadband seismic networks: Project Geoscope, IRIS/USGS, IRIS/IDA, CDSN, GDSN, and the IRIS Data Management Center. Michelle Kuth and Liqiang Su aided our acquisition and selection of Geoscope data. This work has been supported by NSF grants EAR-9018215, EAR-9018442, and EAR-9219367.

## References

Anderson, D. L., *A Theory of the Earth*, pp. 303-333, Blackwell Scientific, Boston, Mass., 1989.

Backus, G. E., Possible forms of seismic anisotropy of the uppermost mantle under oceans, *J. Geophys. Res.*, *70*, 3429–3439, 1965.

Christensen, N. I., The magnitude, symmetry and origin of upper mantle anisotropy based on fabric analyses of ultramafic tectonites, *Geophys. J. R. Astron. Soc.*, *76*, 89–111, 1984.

Crampin, S., A review of the effects of anisotropic layering on the propagation of seismic waves, *Geophys. J. R. Astron. Soc.*, *49*, 9-27, 1977.

Dziewonski, A. M., A. L. Hales, and E. R. Lapwood, Para-

metrically simple Earth models consistent with geophysical data, *Phys. Earth Planet. Inter.*, *10*, 12–48, 1975.

Fischer, K. M., K. C. Creager, and T. H. Jordan, Mapping the Tonga Slab, *J. Geophys. Res.*, *96*, 14403-14427, 1991.

Galea, P., Upper mantle anisotropy in the S.W. Pacific from earthquake travel-time analysis, *Phys. Earth Planet. Inter.*, *76*, 229-239, 1993.

Giardini, D., and J. H. Woodhouse, Horizontal shear flow in the mantle beneath the Tonga arc, *Nature*, *319*, 551-555, 1986.

Hager, B., and R. O'Connell, Kinematic models of large-scale flow in the Earth's mantle, *J. Geophys. Res.*, *84*, 1031-1048, 1979.

Karato, S., M. S. Paterson, and J. D. F. Gerald, Rheology of synthetic olivine aggregates: Influence of grains-size and water, *J. Geophys. Res.*, *91*, 8151-8176, 1986.

Kato, M., and K. Hirahara, Anomalous propagation of Rayleigh waves along Izu-Mariana trench, *Geophys. Res. Lett.*, *19*, 2333-2336, 1992.

Kawasaki, I., and K. Koketsu, Rayleigh-Love wave coupling in an azimuthally anisotropic medium, *J. Phys. Earth*, *38*, 361-390, 1990.

Kirkwood, S., and S. Crampin, Surface-wave propagation in an ocean basin with an anisotropic upper mantle: Numerical modeling, *Geophys. J. R. Astron. Soc.*, *64*, 463-485, 1981a.

Kirkwood, S., and S. Crampin, Surface-wave propagation in an ocean basin with an anisotropic upper mantle: Observations of polarization anomalies, *Geophys. J. R. Astron. Soc.*, *64*, 487-497, 1981b.

Kuo, B.-Y., and D. W. Forsyth, A search for split SKS waveforms in the Pacific, *Geophys. J. Int.*, *108*, 557-574, 1992.

Lay, T., J. W. Given, and H. Kanamori, Long-period mechanism of the 8 November 1980 Eureka, California, earthquake, *Bull. Seismol. Soc. Am.*, *72*, 439-456, 1982.

Mainprice, D., and P. G. Silver, Constraints on the interpretation of teleseismic SKS observations from kimberlite nodules from the subcontinental mantle, *Phys. Earth Planet. Inter.*, *78*, 257-280, 1993.

Masters, G., J. Park, and F. Gilbert, Observations of coupled spheroidal and toroidal modes, *J. Geophys. Res.*, *88*, 10285–10298, 1983.

Masters, T. G., Low-frequency seismology and the three-dimensional structure of the Earth, *Philos. Trans. R. Soc. London, Ser. A*, *328*, 329–350, 1989.

McKenzie, D. P., Finite deformation during fluid flow, *Geophys. J. R. Astron. Soc.*, *58*, 689–715, 1979.

McLaughlin, K. L., T. G. Barker, S. M. Day, B. Shkoller, and J. L. Stevens, Effects of subduction zone structure on explosion-generated Rayleigh wave: 3-D numerical simulations, *Geophys. J. Int.*, *111*, 291-308, 1992.

Montagner, J.-P., and T. Tanimoto, Global anisotropy in the upper mantle inferred from the regionalization of phase velocities, *J. Geophys. Res.*, *95*, 4797–4819, 1990.

Montagner, J.-P., and T. Tanimoto, Global upper mantle tomography of seismic velocities and anisotropies, *J. Geophys. Res.*, *96*, 20337–20351, 1991.

Morris, G. B., R. W. Raitt, and G. G. Shor, Velocity anisotropy and delay-time maps of the mantle near Hawaii, *J. Geophys. Res.*, *74*, 4300-4316, 1969.

Nicolas, A., and N.I. Christensen, Formation of anisotropy in upper mantle peridotites: A review, in *Composition, Structure and Dynamics of the Lithosphere-Asthenosphere System, Geodyn. Ser.*, vol. 16, edited by K. Fuchs and C. Froidevaux, pp. 111-123, AGU, Washington, D. C., 1987.

Nishimura, C. E., and D. W. Forsyth, Rayleigh wave phase velocities in the Pacific with implications for azimuthal anisotropy and lateral heterogeneities, *Geophys. J. R. Astron. Soc.*, *94*, 479-501, 1988.

Nishimura, C. E., and D. W. Forsyth, The anisotropic structure of the upper mantle in the Pacific, *Geophys. J.*, *96*, 203-230, 1989.

Park, J., Synthetic seismograms from coupled free oscillations: The effects of lateral structure and rotation, *J. Geophys. Res.*, *91*, 6441–6464, 1986.

Park, J., The sensitivity of seismic free oscillations to upper mantle anisotropy, zonal symmetry, *J. Geophys. Res.*, *98*, 19933-19949, 1993.

Park, J., and F. Gilbert, Coupled free oscillations of an aspherical, dissipative, rotating Earth: Galerkin theory, *J. Geophys. Res.*, *91*, 7241–7260, 1986.

Park, J., and Y. Yu, Anisotropy and coupled free oscillations: Simplified models and surface wave observations, *Geophys. J. Int.*, *110*, 401-420, 1992.

Park, J., and Y. Yu, Seismic determination of elastic anisotropy and mantle flow, *Science*, *261*, 1159-1162, 1993.

Park, J., F. L. Vernon III, and C. R. Lindberg, Frequency-dependent polarization analysis of high-frequency seismograms, *J. Geophys. Res.*, *92*, 12664-12674, 1987.

Peselnick, L., and A. Nicolas, Seismic anisotropy in an ophiolite peridotite: Application to oceanic upper mantle, *J. Geophys. Res.*, *83*, 1227–1235, 1978.

Ribe, N. M., A continuum theory for lattice preferred orientation, *Geophys. J.*, *97*, 199–207, 1989a.

Ribe, N. M., Seismic anisotropy and mantle flow, *J. Geophys. Res.*, *94*, 4213–4223, 1989b.

Ribe, N. M., and U. R. Christensen, Three-dimensional modelling of plume-lithosphere interaction, *J. Geophys. Res.*, *99*, 669–682, 1994.

Ribe, N. M., and Y. Yu, A theory for plastic deformation and textural evolution of olivine polycrystals, *J. Geophys. Res.*, *96*, 8325–8336, 1991.

Russo, R. M., and P. G. Silver, Trench-parallel flow beneath the Nazca Plate from seismic anisotropy, *Science*, *263*, 1105–1111, 1994.

Sandwell, D. T., and W. H. F. Simth, Global marine gravity from ERS-1, Geosat and Seasat reveals new tectonic fabric (abstract), *Eos Trans. AGU*, *73* (43), Fall Meeting Suppl., 133, 1992.

Shearer, P. M., and J. A. Orcutt, Compressional and shear wave anisotropy in the oceanic lithosphere - The Ngendei seismic refraction experiment, *Geophys. J. R. Astron. Soc.*, *87*, 967–1003, 1986.

Su, L., J. Park, and Y. Yu, Born seismograms using coupled free oscillations: The effects of strong coupling and anisotropy, *Geophys. J. Int.*, *115*, 849-862, 1993.

Su, W., and A. D. Dziewonski, Predominance of long-wavelength heterogeneity in the mantle, *Nature*, *352*, 121–126, 1991.

Tanimoto, T., Long-wavelength *S*-velocity structure throughout the mantle, *Geophys. J. Int.*, *100*, 327–336, 1990.

Tanimoto, T., Waveform inversion for three-dimensional density and *S* wave structure, *J. Geophys. Res.*, *96*, 8167–8190, 1991.

Tanimoto, T., and D. L. Anderson, Mapping convection in the mantle, *Geophys. Res. Lett.*, *11*, 287-290, 1984.

Vinnik, L. P., L. I. Makeyeva, A. Milev, and A. Y. Usenko, Global patterns of azimuthal anisotropy and deformations in the continental mantle, *Geophys. J. Int.*, *111*, 433-447, 1992.

Woodhouse, J. H., and A. M. Dziewonski, Mapping the upper mantle: Three-dimensional modeling of Earth structure by inversion of seismic waveforms, *J. Geophys. Res.*, *89*, 5953–5986, 1984.

Woodhouse, J. H., and Y. K. Wong, Amplitude, phase and path anomalies of mantle waves, *Geophys. J. R. Astron. Soc.*, *87*, 753-774, 1986.

Woodward, R. L., and G. Masters, Global upper mantle structure from long-period differential travel times, *J. Geophys. Res.*, *96*, 6351–6378, 1991.

Yu, Y., and J. Park, Upper mantle anisotropy and coupled-mode long-period surface waves, *Geophys. J. Int.*, *114*, 473-489, 1993.

Zhang, Y. S., and T. Tanimoto, High-resolution global upper mantle structure and plate tectonics, *J. Geophys. Res.*, *98*, 9793-9823, 1993.

---

J. Park and Y. Yu, Department of Geology and Geophysics, Yale University, P.O. Box 208109, New Haven, CT 06520-8109. (e-mail: yuyang@hess.geology.yale.edu)

(Received May 17, 1993; revised March 28, 1994; accepted April 5, 1994.)